Zeitschrift: IABSE reports = Rapports AIPC = IVBH Berichte
Band: 999 (1997)

Rubrik: Structural design

Nutzungsbedingungen
Die ETH-Bibliothek ist die Anbieterin der digitalisierten Zeitschriften. Sie besitzt keine Urheberrechte an den Zeitschriften und ist nicht verantwortlich für deren Inhalte. Die Rechte liegen in der Regel bei den Herausgebern beziehungsweise den externen Rechteinhabern. Siehe Rechtliche Hinweise.

Conditions d'utilisation
L'ETH Library est le fournisseur des revues numérisées. Elle ne détient aucun droit d'auteur sur les revues et n'est pas responsable de leur contenu. En règle générale, les droits sont détenus par les éditeurs ou les détenteurs de droits externes. Voir Informations légales.

Terms of use
The ETH Library is the provider of the digitised journals. It does not own any copyrights to the journals and is not responsible for their content. The rights usually lie with the publishers or the external rights holders. See Legal notice.

Download PDF: 22.12.2024

ETH-Bibliothek Zürich, E-Periodica, https://www.e-periodica.ch

Design Guidance for Joints Using Polymeric Composite Materials

J. Toby MOTTRAM
Dr., Senior Lecturer
University of Warwick
Warwick, UK

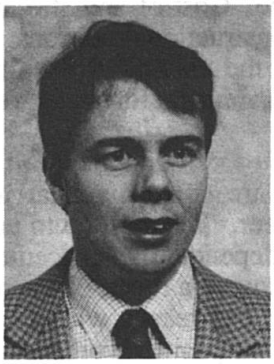

Toby Mottram, born 1958, received his engineering degrees in 1979 and 1984. He has researched polymeric composite materials and structures since 1979. At Warwick University since 1987, his research has focused on framed construction. He is Chairman of DG XII COST C1 material working group.

Summary

A review is presented on design guidance sources for structural joints between members of polymeric composite, and of other materials. Testing, analysis and design for the various types of structural connection are considered. Two principal findings are that; design procedures are more complex than for conventional structural materials; standard joint details are needed to provide end-users with confidence on performance.

1. Introduction

Growth and interest in polymeric composite materials in the building and construction industry occurred initially during the 1960s and 70s. Materials consisted of glass fibre and room temperature curing polyesters, often referred to as glass reinforced polyesters. These were manufactured into curved panels and vessels using contact moulding techniques (Hollaway 1993). Fibre reinforcement was often discontinuous chopped strand mat, at a relatively low volume fraction. To obtain satisfactory strength and stiffness the correct structural form had to be used, and joints, if present, did not transmit appreciable forces (i.e. their purpose was to provide a weather seal).

In the last fifteen years there has been further interest in the use of polymeric composites as different manufacturing processes are exploited (Hollaway 1993, Clarke 1996). Amongst these attractive processes are pultrusion, filament winding, resin transfer moulding, and prepreg moulding. Each process uses different fibre systems with continuous reinforcement, at a relatively high volume fraction, to produce specific structural members and components. Mechanical properties of polymeric composite materials using these processes are therefore higher than those by contact moulding. One advantage of composites over conventional construction materials is the versatility of the different manufacturing processes. In the rest of the paper FRP will be used as shorthand for polymeric composite materials.

Key advantages of FRP are, free-form and tailored design characteristics, high strength-to-weight ratios, and a high degree of corrosion resistance. These are some of the reasons why their use in construction has received increasing attention (Mottram 1995). However, despite the wide use of FRPs in the aerospace industries the civil engineering sector has been slow to take up these materials. There are many in the construction sector who do not have the confidence to use FRPs because of concerns on basic issues relating to the material itself, such as mechanical

properties and modes of failure, durability and fire resistance. However, many of these issues are not such a serious problem as to prevent FRPs from being used, and to educate the construction industry these have in detail been addressed in recent publications (Hollaway 1993, Clarke 1996). There does however remain the problem of cost and this is likely to persist until there is well-established practice and more experience. Cost of any structure is always a major consideration when choosing between different construction solutions. FRPs are expensive materials (on a weight basis) and because of this the reinforcement in more than 90% of applications is glass. The general points given herein are therefore most relevant to joints using glass FRPs.

Those engaged in developing FRPs and structures are conscious that jointing has a special significance and poses a major challenge to the engineer. This has led to pultruders (Anon 1989, 1993, 1995) and others (Clarke 1996) to write, independently, procedures for the structural design of connections. Each design guidance source covers a range of connection types from the list in Table 1. The diversity of guidance available is one reason why this review is timely and within the scope of the activities of the Polymeric Composites working group (1995-); part of the European DG XII project COST C1, 'Semi-rigid behaviour of Civil Engineering Structural Connections' (1991-1999). It is worth noting that none of the sources discussed has any national or international legal standing; there is the expectation that what exists today will form the nucleus for regulatory standards by the next century.

2. Connections

2.1 Classification

The choice of manufacturing processes and the wide range of available fibre reinforcement/polymer resin systems means that the range of structural forms is larger than with concrete, steel and timber (Hollaway 1993, Clarke 1996). Table 1 gives a hierarchic classification of connection types having a potential in construction. As a result of this, there is naturally a larger scope for connection types. The main focus is on FRP to FRP connections because these have received most attention. Some of the design guidance is also appropriate for connections of FRP and steel, FRP and timber, FRP and concrete.

Mechanical joints	Bonded joints	Combined joints	JOINT CATEGORIES
Bolted (shear loaded)	Adhesively bonded	Bonded-bolted	
Bolted (axially loaded)	Laminated	Bonded-riveted	
Riveted (shear loaded)	Moulded		JOINING TECHNIQUES
Riveted (axially loaded)	Cast-in		
Clamped	Bonded insert		
Contact (keyed, hooked)			
Embedded fasteners			
Lap	Lap	Lap	
Strap	Strap	Strap	
Tee	Scarf	Tee	JOINT CONFIGURATION
Angle	Butt	Others	
Others	Tee		
	Angle		
	Others		

Table 1 Classification of connection types (from Clarke 1996)

Classification is also dependent on the function of the joint in the structure. Connections are therefore further classified (Clarke 1996) into;

primary structural

secondary structural
non-structural.

We are principally concerned with primary structural where the joint is expected to provide major strength and stiffness to an assembly for the whole life of the structure. The failure of these connections will have a substantial effect on the performance of the whole structure. Such connections will carry the highest requirement for strength, stiffness and durability. Design guidance must be adequate for connections to be safe and reliable over their whole design life.

When the large choice of connection types (Table 1) is linked with the enormous range of FRP mechanical properties it is not surprising that we find design guidance is often limited in scope and, if general, it has only been partially assessed by testing. This is an important observation which engineers need to understand before they apply any guidance appropriate to the specified materials and structural form.

2.2 Research

Prior to the late 1980s the majority of FRP structures had components manufactured by contact moulding. Jointing was generally non-structural or maybe secondary structural. The need to understand the structural behaviour of these connections was limited and they did not receive much attention. Only a handful of technical papers on FRP joints were published prior to this time (Heger 1984, Mottram 1995).

The interest in structural members made by pultrusion saw the need for research on the performance of primary structural connections. Studies made by academics include extensive laboratory testing and numerical simulation. The objective has been to provide data for the development of design guidance. Between 1980 and 1989 a single conference paper was published. The number of publications has increased significantly in the 1990s with to date over 30 conference and 20 journal papers. Most of the research has been with bolted joints (lap and tee joint classification). Much of the recent work has not yet been used by those involved in writing design guidance.

Hutchinson (1997) has prepared a state-of-art report to review all aspects of joining FRPs in construction. Chapter 5 on 'Joint Design Approaches' has a section where Hutchinson compares recent recommended fastener distances for pultruded lap-joints with those previously known (Anon 1989, Clarke 1996). One interesting feature of the report is that Chapter 8 gives case studies of joints. It was expected that the case studies would refer to the design guidance in Chapter 5. However, Hutchinson found that full details on how each joint was designed were absent when the structure was reported; this a consequence of the commercial nature of these new construction technologies.

3. Design Guidance for Joints

3.1 Europe

The two sources of design guidance (Anon 1995, Clarke 1996) use the limit state approach (Head 1994). They are different and specific details are not within the scope of the paper.

In 1995 the pultruders Fiberline Composites A/S released their design manual (Anon 1995). The limit state approach adopted by the Company uses partial safety factors for material strengths and stiffnesses in order to conform the dimensioning to Danish Standard 456. A design procedure is presented for flat panels (thickness 3 to 20 mm) fastened by steel bolts (M6 to M48) in a lap-joint configuration. Loading is in the plane of joint. Simple design equations are given to determine the joint's ultimate resistance. Of the five different modes of failure used in the design procedure two have new theoretical models that, to the author's knowledge, have not been reported elsewhere. The manual presents tables of design values (load capacity (kN)) in the

longitudinal and transverse material directions to enable engineers to design their own bolted connections of the types listed in Table 1. A number of worked examples (e.g. lap, tee, angle joints) illustrate how the tables can be used.

Testing was conducted to determine the characteristic material strengths needed in the design equations. The Fiberline Design Manual does not provide reference to any joint test results. There are no recommendations for jointing by adhesive bonding.

The first independent, practical source of guidance on structural connections is given in the EUROCOMP Design Code (Clarke 1996). Chapter 5 deals with the problem of designing efficient, safe and reliable connections. It is recognised that FRPs differ from conventional materials in that adhesive bonding is used to form primary structural joints. Many of the fundamental principles used to develop the procedures was due to technology transfer from aerospace companies in America.

The code provides guidance for inplane loaded joints where the joined members are flat panels. The guidance is for general application. At the ultimate limit state a simplified approach is given for bolted and bonded joints. A more rigorous design procedure is provided for bonded joints. The equivalent procedure for bolted joints relies on proprietary finite element software (BOLTIC 1996) and is detailed in the background part of the book. It does not appear in the code because the EUROCOMP partners felt that it had not been sufficiently proven. Both rigorous design approaches use analyses that allow the joint response to be semi-rigid.

All design procedures have to consider the problem of predicting, to acceptable accuracy, the effect on joint resistance of local stress fields. These occur for example in a panel in the region adjacent to the boundary between a bolt and FRP material. A solution is by finite element analysis (BOLTIC 1996). Such a problem is not as serious when the panel is of steel because yielding relieves such stress 'hot spots'. This single factor ensures that design for FRP connections requires special attention and is one reason why good design guidance remains limited. It also means that compliance testing of a new connection design will remain important, and it will often be a necessary stage in the design process. The code recommends this approach.

Partial safety factors listed for the design approaches are based on the collective experience of the EUROCOMP code writers. The code provides guidance to check serviceability of connections.

The EUROCOMP code does not formally cover tee joints (e.g. beam-to-column) that are routinely used in framed construction. One of the test reports by Mottram (Clarke 1996) does present test results that are used to make simple design guidance for nominally pinned beam-to-column connections. Details of the five connections tested are to be found in the MMFG design manual (Anon 1989). This research, and that on the development of practical tee joint connections for frames to be designed as semi-rigid is discussed by Mottram and Zheng (1997). Understanding of this connection type is still at a low level and so design guidance is limited to simple connections.

Followers of the use of FRPs in construction will undoubtably have knowledge of the advanced composite construction system developed by Maunsells and Partners, UK (Hollaway 1993). This innovative system has joints formed by the mechanical interlocking of pultruded sections. Adhesive bonding is often used to improve connection performance. For commercial reasons details of the jointing method are not available and design guidance on this method has not been developed by others. The Company has its own limit state design approach (Head 1994).

3.2 American

The first design manual for pultruded structurals was prepared in 1971 by the world's largest pultruder Morrison Molded Fiber Glass Co. A major revision was started in 1983 representing years of manufacturing experience, monitoring applications and extensive product testing. The current manual was released in 1989 and is periodically updated. This manual (Anon 1989) uses the American stress allowable design approach and gives guidance for designing simple frames (braced). Recommended details are given for pinned framed connections with the principal method of connection by bolts (FRP). The dimensions of the connection pieces mimic practice seen in steelwork. The manual also recommends that best joint performance is obtained by combined bolting and bonding. The manual does not give access to the Company's extensive product testing. Results by academics of tests on MMFG's connection details were first published in 1990 (see Mottram and Zheng 1997) and this research is continuing.

In 1984 the American Society of Civil Engineers (ASCE) published their Structural Plastics Design Manual because its members could see these emerging materials as amongst the most promising and potentially useful to the engineering profession. The design manual funded by industry and government was a necessary step in overcoming the major unresolved problems of using the materials. Of the 1176 pages comprising the manual just 25 are on joints or connections. Little design guidance is provided and that which is relies on recommendations developed for marine applications in the early 1960s. This deficiency of the manual is recognised and in the Foreword it states "The Connection's-Fastening Committee is in the process of preparing proposals for solicitation from interested parties that would undertake the development of a manual covering this subject." No such ASCE manual has been published and to the author's knowledge its preparation is not well advanced. Within the Materials Division there is a Technical Committee on Structural Composites and Plastics (known as SCAP) that is involved in promoting the preparations of ASCE prestandards and standards.

R.E.Chambers of Chambers Engineering, Canton, Ma, started in 1996 a project to prepare the ASCE/PIC Prestandard 'Load and Resistance Factor Design (LRFD) Standard for Structural Pultruded Fiber Reinforced Plastic (PFRP) Rods, Plates and Shapes'. This will, for mechanical fastened connections, give design guidance similar to Fiberline (Anon 1995). There will also be an introduction to tee joint details for framed construction based on the novel universal connector piece developed by Mosallam in America (Anon 1993, Mottram and Zheng 1997).

4. Conclusions

Analysis of the design guidance sources and background information would led to the following general conclusions:

i) Connections between polymeric composite materials are generally by adhesive bonding or mechanical fastening (usually bolted), and their design is significantly more difficult than for connections between other construction materials.
ii) Connections for plate-to-plate and plate-to-structure (e.g. bonding of thin laminates to existing concrete/masonry structures) are the joint types preferred because the moment transmitted is low.
iii) Technology transfer from the aerospace industry has enabled there to be standard test methods, rigorous analytical and design tools for the structural design of bonded and bolted plate-to-plate connections (e.g., lap and strap joints).

iv) There is an urgent need for the available design procedures to be verified by research to ensure the reliability of 'safe' connections. Rigorous design procedures for bonded and bolted connections do consider the joint to behave with semi-rigid action.
v) Mechanical interlocking joints (bonding an option) are used successfully in practice. Their performance and design guidance remain restricted to commercial organisations.
vi) Connections for framed structures are not found in aerospace applications and so engineers have had little experience of how to use them in practice. Research is on-going to develop pieces and details for simple and semi-rigid connections for frames of pultruded members. Design guidance is very limited.
vii) Lack of 'ductility' of FRPs, and of certain adhesive systems, means that local analysis of stresses is very important, and this aspect of FRP connections make reliable design guidance, particularly for long-term loadings, much more difficult to develop than for other materials.
viii) The majority of the testing and analysis has been for connections between members of FRPs (and often the same material) that are plate-to-plate (lap joints).
ix) Research is needed to establish the reliability of all connection types, with particular reference to the variability in stiffnesses and strengths, etc. Understanding is also needed to develop standard products and modular systems, such that FRP frames with integral semi-rigid joints can be designed with the same degree of confidence as for steel.
x) The details of bolted and bonded connections often mimic those in steel practice and these joints do not necessarily use polymeric composite properties efficiently. There is therefore a need to create second generation connection designs to promote better use of the material.
xi) Interested parties should take existing design guidance and other information and prepare standards of legal standing.

References

Anon, (1989). *'EXTREN Design Manual'*. Morrison Molded Fiber Glass Co. (MMFG), Bristol, Va, USA. (Addendum 1990 & 1995.)
Anon, (1993). *'BRP Design Guide'*, Bedford Reinforced Plastics, Inc., Bedford, Pa, USA.
Anon, (1995). *'Fiberline Design Manual for Structural Profiles in Composite Materials'*, Fiberline Composites A/S, Kolding, Denmark.
Clarke, J.L., (Ed.), (1996). *'Structural Design of Polymeric Composites - EUROCOMP Design Code and Handbook'*, E & FN Spon, London.
Head, P.R., (1994). 'Limit State Design Methods', Chapter 7, in Hollaway, L. (Ed.), *'Handbook of Polymer Composites for Engineers'*, Woodhead Publ. Co. and BPF, Cambridge, 181-197.
Hollaway, L., (1993). *'Polymer Composites for Civil and Structural Engineering'*, Blackie Academic & Professional, Glasgow.
Hutchinson, A.R., (1997). *'Joining of Fibre Reinforced Polymer Composite Materials'*, CIRIA RP 515, CIRIA, London. (Core programme members.)
Mottram, J.T., (1995). 'Pultruded profiles in construction: A review,' in Bank, L.C., and Ben-Bassat, M., (Eds.), *The 1st Israeli Workshop on Composite Materials for Civil Engineering Construction'*, NBRI, Haifa, Israel, 28-29 May 1995, NBRI, 152-180.
Mottram, J.T., and Zheng, Y., (1997). 'State-of-the-art review on the design of beam-to-column connections for pultruded frames', *Composite Structures*, p.15, *to be published.*
Heger, F.J., Chambers, R.E., and Dietz, A.G.H., (1984). *'Structural Plastics Design Manual'*, ASCE Manuals and Reports on Engineering Practice No. 63, ASCE, NY.
BOLTIC User's Guide (1996), A Program for Strength Analysis of Composite Bolted Joints, Department of Lightweight Structures, Royal Institute of Technology, Sweden.

The Design for Local Buckling of Concrete Filled Steel Tubes

Martin O'SHEA
Research Fellow, Civil Engineering
University of Western Sydney
Sydney, Australia

Russell BRIDGE
Professor of Civil Engineering
University of Western Sydney
Nepean, Australia

Summary

From the analysis of carefully controlled experiments, the influence of local buckling on the behaviour of short circular thin-walled concrete filled steel tubes has been examined. Two possible failure modes of the steel tube have been identified, local buckling and yield failure. These were found to be independent of the diameter to wall thickness ratio. Instead, bond (or lack of it) between the steel and concrete infill determined the failure mode. A proposed design method has been suggested based upon the recommendations in Eurocode 4 (1992).

1. Introduction

Circular concrete filled steel tubes have been found to be an economical column alternative (Watson and O'Brien, 1990). Further economies are possible if high strength concrete infill is used in conjunction with thin-walled steel tubes, with just sufficient steel to support the floors while under construction (Webb and Peyton, 1990).

It has been recognised that the capacity of thin-walled circular steel tubes may be reduced by local buckling effects, with their post ultimate response exhibiting little ductility. Conservative predictions of the local buckling strength can be made using currently available design methods (O'Shea and Bridge, 1996) such as AISI-LRFD (1991) and AISC-LRFD (1994) while the unloading response is dependent upon the specimen length. The behaviour of high strength concrete has also been shown to exhibit a rapid unloading response in the postultimate region with strain reversal evident at strengths of 115 MPa (O'Shea and Bridge, 1994). For thick-walled steel tubes filled with low to medium strength concrete, enhancement of the concrete has been found to occur for short axially loaded specimens due to the confining pressures exerted by hoop stress in the steel tube. However, this then reduces the axial capacity of the steel tube which is recognised in Eurocode 4. For thin-walled circular concrete filled steel tubes, both hoop stress and local buckling effects have to be considered. Due to these effects, the summation of the individual ultimate strengths of the steel and the concrete, even taking strain compatibility into account, is not likely to be appropriate or valid for design purposes. As few tests have been carried out on axially loaded thin walled concrete filled steel tubes, tests were performed to evaluate the issues identified above.

2. Axially Loaded Steel Tubes

Ten axially loaded steel tubes were examined with properties as shown in Table 1. Five diameter to thickness ratios (D/t) were selected. The specimens were all short with a length (L) to diameter ratio of 3.5. Material coupon tests were conducted to determine yield strength (f_y) and elastic modulus (E_s). Two series of tests were performed. In the series labelled BS, the specimens were axially loaded with no internal restraint. In the other series labelled BSC, the specimens were filled with unbonded concrete to restrain the possible formation of internal buckles. The local strains in the steel tube were measured using three internal and external strain rosettes placed at midheight.

Specimen	D (mm)	t (mm)	D/t	f_y (MPa)	E_s (MPa)	L (mm) BS	L (mm) BSC	Strength (kN) BS	Strength (kN) BSC
S30	165	2.82	58.6	363.3	200600	580.0	575.0	522.6	n.a.
S20	190	1.94	98.2	256.4	204700	665.0	657.0	284.4	279.9
S16	190	1.52	125.1	306.1	207400	665.0	657.5	239.2	283.8
S12	190	1.13	168.1	185.7	178400	665.0	659.5	109.1	109.3
S10	190	0.86	220.4	210.7	177000	665.0	658.5	92.9	91.0

n.a. not available

Table 1 Test results for axially loaded steel tubes

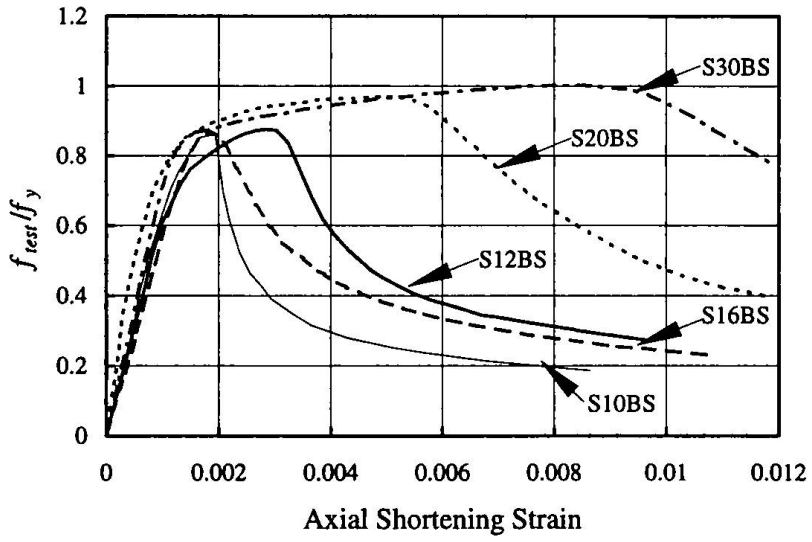

Figure 1 Normalised load axial shortening response for axially loaded unfilled steel tubes

The normalised load axial shortening curve for the BS specimens has been included in Figure 1 where f_{test} is the experimentally applied stress. For clarity the BSC specimens have not been included as they exhibited an experimentally similar response. This can also be seen in the principal strains for specimen S10 in Figure 2 with both S10BS and S10BSC having the same strain response. The elastic unloading of the tube in the post ultimate region can be clearly seen with the vertical and circumferential strains reducing. For this to occur the axial shortening must occur in the locally buckled region. The ultimate strengths of the companion BS and BSC tubes in Table 1 are similar. Consequently the internal concrete was found to have no influence on the buckling mode of the axially loaded steel tube. The only exception was specimen S16BSC. In this case the local buckle occurred at mid-height compared to an end for all other specimens.

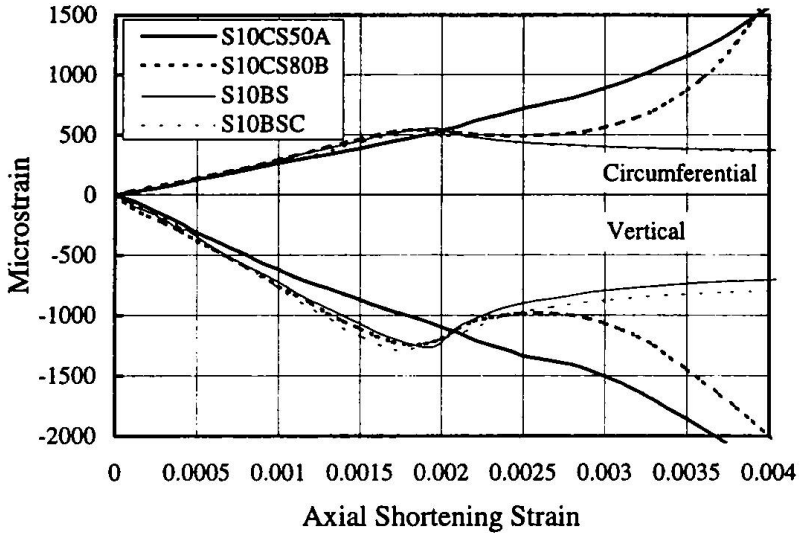

Figure 2 Local strains for Specimen S10BS, S10BSC, S10CS50A and S10CS80B

The incremental Poisson's ratio for each specimen was calculated from the principal vertical and circumferential strains. Three curves of best fit, reflecting the different material properties were obtained as in Figure 3. An upper limit of 0.5 was used to indicate full plasticity.

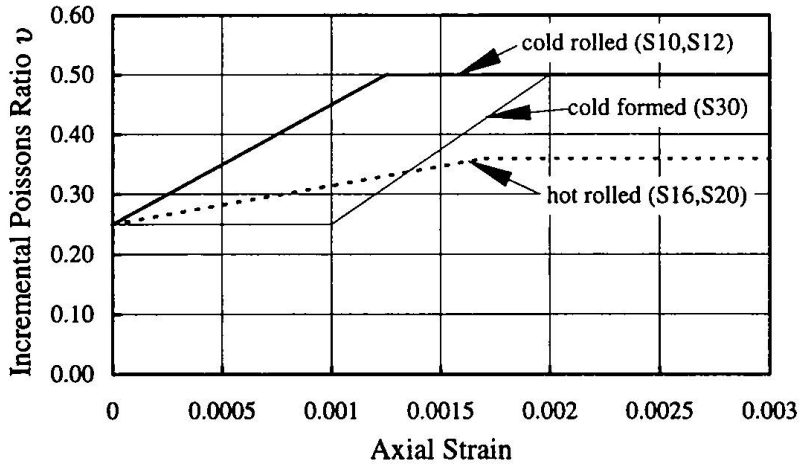

Figure 3 Poisson's ratio used in the analysis

3. Axially Loaded Concrete Filled Steel Tubes

Ten concrete filled steel tubes (CFT) labelled CS were tested with dimensions as shown in Table 2. They were identical to their companion axially loaded steel tubes but were filled with concrete. Two nominal concrete strengths of 50 or 80 MPa were selected with two mixes of each type. After filling, the CFT ends were sealed with plastic and stored in the concrete laboratory at ambient room temperature until testing. Ten 100 mm diameter material property cylinders were cast for each mix. After demoulding, half the material cylinders were stored in a lime bath at a constant temperature of 20 degrees, the rest were sealed in plastic and stored with the tubes. The latter were used for the indicative concrete properties, strength (f_c) and elastic modulus (E_c), as the CFT environment was accurately simulated. Prior to testing, the specimen ends were ground

square and flat to ensure that the steel and concrete were loaded together. Three strain rosettes evenly spaced at midheight were attached to each CFT.

Specimen	D (mm)	t (mm)	D/t	L (mm)	f_c (MPa)	E_c (MPa)	f_y (MPa)	E_s (MPa)	Strength (kN)
S30CS50B	165	2.82	58.6	580.5	48.3	21210	363.3	200600	1662
S20CS50A	190	1.94	98.2	663.5	41.0	17810	256.4	204700	1678
S16CS50B	190	1.52	125.1	664.5	48.3	21210	306.1	207400	1695
S12CS50A	190	1.13	168.1	664.5	41.0	17810	185.7	178400	1377
S10CS50A	190	0.86	220.4	659	41.0	17810	210.7	177000	1350
S30CS80A	165	2.82	58.6	580.5	80.20	28450	363.3	200600	2295
S20CS80B	190	1.94	98.2	663.5	74.7	27580	256.4	204700	2592
S16CS80A	190	1.52	125.1	663.5	80.2	28450	306.1	207400	2602
S12CS80A	190	1.13	168.1	662.5	80.2	28450	185.7	178400	2295
S10CS80B	190	0.86	220.4	663.5	74.7	27580	210.7	177000	2451

Table 2 Test results for axially loaded concrete filled steel tubes

Two different failure modes were observed from the tests. In yield failure, bond between the steel and the concrete was maintained. This can be observed in Figure 2 for specimen S10CS50A with the principal strains increasing with axial shortening strain. However in buckling failure, bond was not maintained with local buckling of the steel occurring as in specimen S10CS80B in Figure 2.

4. Analysis of Tests

An incremental elastic analysis was chosen to determine the vertical stress and the hoop stress from the measured strains. A failure surface defined by the maximum energy distortion theory (Higdon et. al., 1977) was used. The intersection point with the failure surface was assumed to remain constant with increasing axial shortening strain.

The response of the confined concrete was calculated by subtracting the steel load component in the vertical direction from the applied load. The peak confined concrete strength (f_{cc}) has been included in Table 3 and plotted in Figure 4 and 5, normalised with concrete strength (f_c). Clearly the nominal 50 MPa concrete has had significant improvement in strength and ductility while for the 80 MPa mix this only occurred for the thicker tubes. Ductility improvement compared to the unconfined behaviour is clearly visible in Figure 5, especially for specimen S30CS80A. An unexpected result occurred for specimen S10CS80B with a high confined concrete strength. However, this was due to buckling of the steel tube allowing greater confinement of the concrete to occur in the elastic region away from the locally buckled region.

From Table 3, Eurocode 4 generally provides a good prediction of the enhanced concrete strength. However a conservative estimate of the vertical steel strength was obtained from Eurocode 4. The inclusion of local buckling as recommended by Eurocode 4 would yield even more conservative results. The high axial steel strengths obtained in the CS tests were due to the influence of bond. This forces the steel to yield by preventing local buckles. If one does form as in specimen S10CS80A then a *higher* axial load can be obtained as greater confinement is possible. This is supported by Orito et. al. (1987) with tests on unbonded concrete filled tubes.

Specimen	Steel reduction f_{test}/f_y			Concrete enhancement f_{cc}/f_c		CS Test / EC 4		
	CS test	BS test	EC 4	CS test	EC 4	Steel	Concrete	Composite
S30CS50B	0.91	1.00	0.80	1.24	1.42	1.14	0.87	0.93
S20CS50A	0.94	0.97	0.80	1.26	1.21	1.18	1.04	1.06
S16CS50B	0.87	0.87	0.80	1.09	1.16	1.09	0.94	0.96
S12CS50A	0.94	0.88	0.80	1.11	1.08	1.17	1.02	1.04
S10CS50A	0.87	0.86	0.81	1.11	1.07	1.07	1.03	1.03
S30CS80A	0.92	1.00	0.81	1.18	1.24	1.14	0.95	0.96
S20CS80B	n.a.	0.97	0.81	1.13	1.11	n.a.	1.02	1.04
S16CS80A	n.a.	0.87	0.81	1.06	1.10	n.a.	0.97	0.99
S12CS80A	0.92	0.88	0.81	0.98	1.04	1.13	0.95	0.95
S10CS80B	0.73	0.86	0.82	1.14	1.04	0.90	1.10	1.09

n.a. Not available

Table 3 Comparison of tests to Eurocode 4 (EC 4)

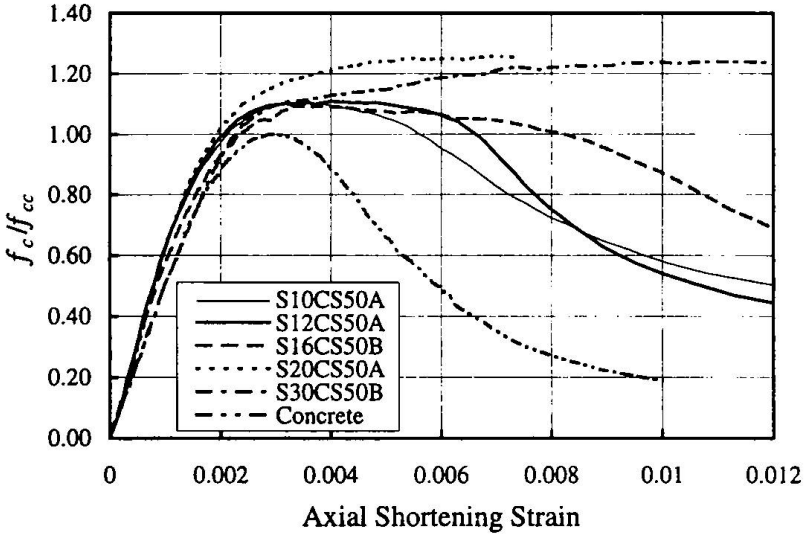

Figure 4 Confined concrete response for nominal 50 MPa mix

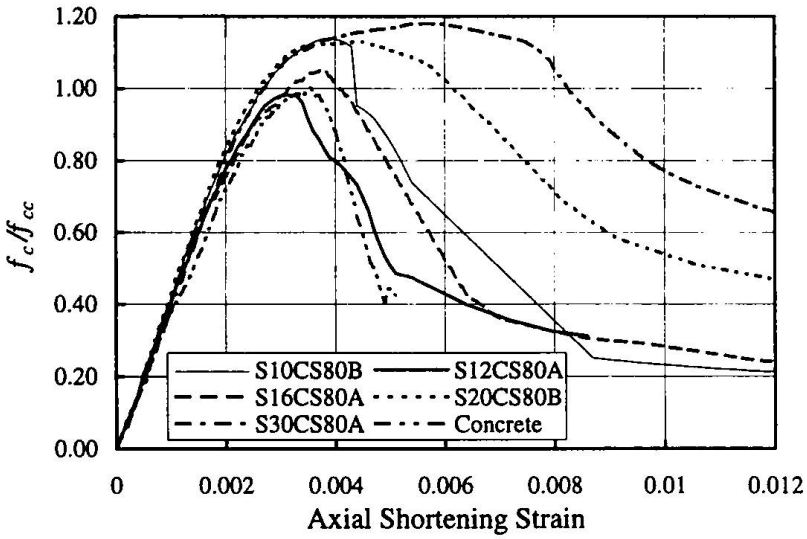

Figure 5 Confined concrete response for nominal 80 MPa mix

5. Conclusions

The ductility of high strength concrete can be significantly improved from the confining action of thin-walled circular steel tubes. Enhancement of the concrete can occur for some combinations of *D/t* ratio and concrete strength. Failure of the steel tube can occur by yielding or buckling. In yield failure, the steel tube reaches yield with the vertical capacity reduced by confining action. In buckling failure, the bond between the steel and concrete is not maintained allowing greater concrete confinement and capacity. Eurocode 4 accounts for both effects giving conservative results for thin-walled tubes filled with concrete. Less conservative predictions can be obtained by excluding the influence of local buckling.

6. Acknowledgements

This support of the following organisations is gratefully acknowledged: Australian Research Council; BHP Steel; Connell Wagner; Boral Research Laboratory; Palmer Tubemills and the School of Civil Engineering at the University of Sydney.

7. References

AISC-LRFD (1994) *Metric Load and Resistance Factor Design Specification for Structural Steel Buildings*, American Institute of Steel Construction, 1st edition, 1994.

AISI-LRFD (1991) *Cold-Formed Steel Design Manual*, American Iron and Steel Institute, 1991.

Eurocode 4 (1992) *ENV 1994-1-1 Eurocode 4, Design of composite steel and concrete structures*, Brussels, European Committee for Standardisation.

Higdon, A. , Ohlsen, E.H. et. al. (1977) *Mechanics of Materials, SI Version, 3rd Edition*, John Wiley and Sons, pp. 483-494.

Orito, Y., Sato, T., et. al. (1987) Study on the Unbonded Steel Tube Concrete Structure, *Proceedings*, Composite Construction in Steel and Concrete, ASCE, New England College, Henniker, New Hampshire, June 7-12, 1987, pp. 786-804.

O'Shea, M.D. and Bridge, R.Q. (1994) Tests of thin-walled concrete filled steel tubes, *Proceedings*, 12th International Speciality Conference on Cold-Formed Steel Structures, St. Louis, Missouri, USA, October 18-19, pp. 399-419.

O'Shea, M.D. and Bridge, R.Q. (1996) Circular thin-walled tubes with high strength concrete infill, *Proceedings*, Composite Construction 3, Engineering Foundation Conference, Germany.

Watson, K.B. and O'Brien, L.J. (1990) Tubular composite columns and their development in Australia, *Proceedings*, 2nd National Structures Conference, Institution of Engineers, Australia, 186-190.

Webb, J. and Peyton, J.J. (1990) Composite concrete filled steel tube columns, *Proceedings*, 2nd National Structures Conference, Institution of Engineers, Australia, 181-185.

Design Basics of a Continuous Composite Slab with Unbonded Tendons

Heli KOUKKARI
MSc. Eng.
VTT Building Technology
Espoo, Finland

Heli Koukkari, born 1953, received her civil engineering degree at Helsinki University of Technology 1979. She joined VTT 1982 and has specialised in composite construction since 1989.

Summary

Theoretical and experimental research on steel-concrete composite slabs with unbonded tendons shows that a composite slab with horizontal shear resistance high enough to withstand the shear induced during the post-tensioning work can be analyzed using the principles developed for post-tensioned concrete slabs in addition that horizontal shear should be checked as a possible failure state. The steel sheet can be fully utilised in the calculations of the effective stiffness and the flexural resistance of the composite slab.

1 Background

At the VTT Building Technology, Finland, a theoretical and experimental research project was undertaken on post-tensioned composite slabs during the years 1994-1996. The purpose of the project was to present the principles of design with respect to resistances at the failure states and performance at the service state.

Prestressing is a powerful method to improve the performance of a composite slab at the service state. Cracking and deflections decreases and flexural stiffness increases by prestressing. These benefits can be utilized in different ways depending on the requirements of an actual building: span lengths can be substantially longer, slab depths can be smaller and a slab can be built in a more severe athmosphere. The benefits from a steel sheet are that it is used as a formwork and it can be used as a substitution of reinforcement necessary as minimum reinforcement and a means to reduce the weight of the floor. It also increases the stiffness of a cracked section.

As a in-situ construction method itself, composite contruction can benefits most from prestressing techniques suitable for building site. For this reason, the research project focused on the post-tensioning methods, especially with unbonded tendons which have small measures in anchorages and sheatings and are finished without grouting (Fig.1).

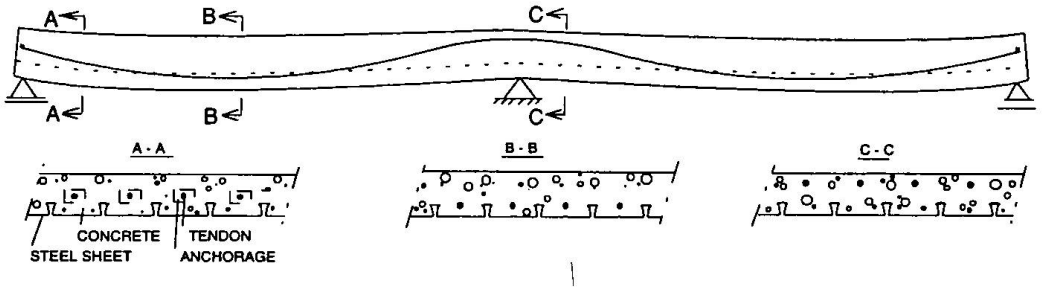

Fig.1. A composite slab with parabolic unbonded tendons.

2 Load balancing approach

The load-balancing approach has been presented by T.Y. Lin and N.H. Burns [3]. It gives a quick and reliable method to calculate the stresses caused by prestressing in any type of structure.

A curved prestressing tendon induces both horizontal and vertical components of the tendon force. The vertical components of a parabolic tendon can be supposed to be uniformly distributed along the length of the slab with the magnitude of

$$w = \frac{8Ph_f}{L^2}$$

where w is the uniformly distributed vertical components of the tendon force
P the tendon force
h_f sag (drape) of the tendon
L the horizontal length of the parabola.

This simple equation is based on a close similarity of a parabola with a circle and small angles between the parabola and the line connecting the ends of the parabola. In a continuous composite slab, the vertical components along the whole length of the slab can be calculated separately for each different parts of parabolas by the aid of the same formula. When the vertical components upwards are as great as the acting loads, the slab is load-balanced. Such a composite slab is purely compressed due to the horizontal component of the tendon force which roughly equals to that.

Prestressing induces support reactions in a continuous slab which in turn induces secondary effects. The bending moment $M_w(x)$ caused by the vertical component of the tendon force is the total internal moment due to the prestressing, and the common methods for continuous beams can be used in calculation of the diagram. The prestressing force causes a primary bending moment $M_1(x)$ in each section. The secondary bending moment $M_2(x)$ is the difference between the total and primary internal bending moments. The secondary moment is needed for the assesment of the secondary support reactions caused by the prestressing.

3 Flexural stresses in a continuous composite slab

The cross-sectional values of a composite slab with unbonded tendon can be calculated by transforming all bonded reinforcement to concrete by the relation of the elastic modules.

$$A_m = \sum n_k A_k$$
$$I_m = \sum \left(n_k I_k + n_k A_k e_k^2 \right)$$

where k the structural part (c refers to concrete, s to rebars and a to steel sheet)
A_k the area of a structural part
I_k the second moment of area of a part with respect to its own centroid
e_k the distance between the centroidal axes of the part and the composite slab
$n_k = E_k/E_c$

In a cracked section, only the compressed concrete is taken into account. The stiffnesses of the uncracked and cracked sections are calculated by multiplying the second moment areas of transformed sections by the elastic modulus of concrete.

The flexural stresses of a continuous slab can be calculated as a sum of the stresses due to the tendon force P, the total bending moment M_w caused by the prestressing and the bending moment caused by the self-weight and other gravity loads, M_p.

$$\sigma = -\frac{P}{A_m} - \frac{M_w}{I_m} y + \frac{M_p}{I_m} y$$

where y the distance from the cetroidal axis of the composite slab to the level of calculation

and the other symbols are given in the formulae above.

4 Shear stresses in the joint

The composite action between the concrete and the steel sheeting was investigated by column tests simulating a balanced composite slab and by push-out tests simulating a joint in a bent slab. A full-scale loading test on a continuous post-tensioned composite slab was also carried out in order to verify the calculation model developed on the basis of balanced load approach and small-scale tests.

Shear stresses are induced in a load-balanced composite slab in the joint due to the transfer of the tendon force in the steel sheeting. This happens in a short anchorage zone where also the tendon force acting locally transfers to a uniform compression of the concrete (Fig. 2a). The composite action in compression was studied by the aid of loading tests on short columns with steel sheetings on two opposite edges. No stirrups were placed in specimens because the calculated failure load of the concrete part was higher than the force needed to cause a compressive stress of 7 N/mm^2, when usually the sustained compressive stresses vary from 1 to 2.5 N/mm^2 in prestressed slabs (Figs. 2b and 2c).

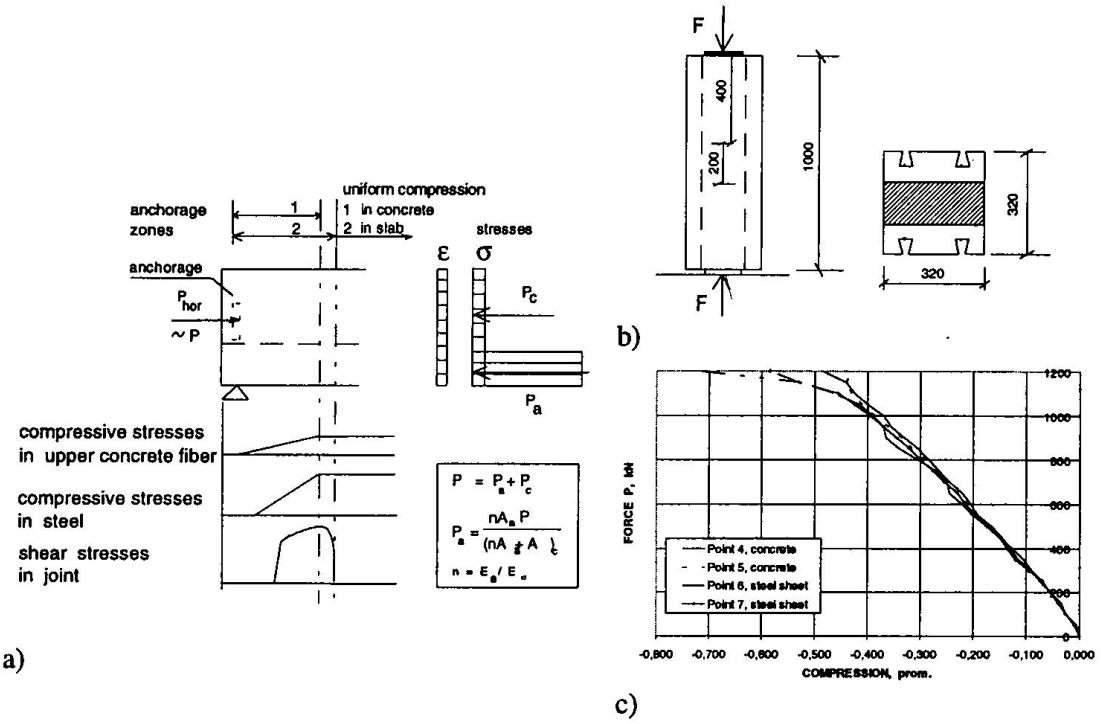

Fig. 2. a) Schematical presentation of transfer of tendon force in the concrete and steel sheeting. b) Compressive tests on short columns c) Results from a compressive test on a short column.

The capability of the joint to transfer the compression force from anchorage to the steel sheeting should be experimentally verified for each type of composite slab. This is due to the short transfer length and relatively high shear stresses which increase with time.

5 Effect of time on a prestressed composite slab

The distribution of stresses varies during the lifetime of a composite slab due to the time-dependence of the stress-strain relations of concrete and prestressing steel, shrinkage of the concrete and composite action between the concrete and steel sheeting. In a composite slab, the continuous change of stresses and strains cause a continuous change in the location of the centroidal axis and stiffnesses, too. For this reason, the cross-sectional values are calculated for all the different times of consideration.

The estimation of the creep of a composite slab happens usually according to the methods generated for concrete structures. The creep is dependent on the measures and surrounding of the slab as well as the time of loading. The relaxation properties of a tendon are defined experimentally.

The shrinkage and creep are restricted by the steel sheeting. This induces additional bending moments and normal forces in the composite slab. However, in a post-tensioned composite slab these additional effects are small. At first, the distance between the centroidal axis of the totally or nearly uncracked concrete part and that one of the composite slab is small and secondly, the permanent load causing creep is usually balanced.

The shear stresses at the ends of the slab gradually increases due to the increase of the share of the tendon force carried by the sheeting, but decreases at the same time due to the losses of the tendon force. The unbalanced loads induces the shear stresses opposite to the stresses induced by the tendon force.

A calculation model was developed for the analysis of the long-term deformations of a composite slab withunbonded tendons in the project at VTT Building Technology. The work was undertaken by modifying the composite slab program CompCal of the Technical University of Lausanne, Switzerland. The performance of the programme has been verified for the ordinary slabs in Lausanne and for the short-term behaviour of a prestressed composite slab at VTT. The creep and shrinkage properties of concrete were programmed according to the widely used expressions presented in CEB-FIP Model Code for concrete structures [1]. The calculated examples show that the long-term deflections will be substantially reduced by post-tensioning [3].

6 Results from a full-scale loading test

A full-scale loading test was undertaken on a continuous composite slab with unbonded tendon with eight line loads (Fig. 3). The width of the slab was 920 mm. The steel sheeting was manufactured from four pieces: two pieces were connected along the longitudinal centre line and these were laid on the supports. The sheet was not continuous over the middle support. The measures and tendons of the specimen were planned to meet the requirement of balanced load by the aid of hand-calculations and computer programme. The slab type used in the experiment was tested beforehand by the small-scale column and push-out tests. Compressive stresses of concrete of about 3.3 N/mm^2 were caused by four tendons and their anchorages of the type BBR-Cona-Single when the average compressive strength of concrete was measured as 32 N/mm^2.

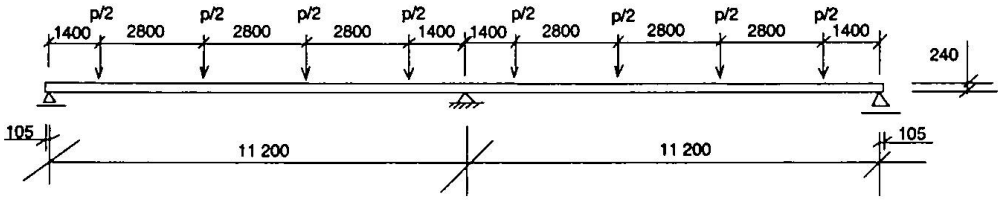

Fig.3. The flexural loading test on a continuous composite slab with unbonded tendons.

The deformations of the specimen were recorded during the tensioning work and the interval between tensioning and loading. There was a cambering of about 2 mm during tensioning which increased 0.2 mm during the first 18 hours. The slip values between the the steel sheet and concrete was recorded during tensioning as 0.07 - 0.11 mm at different points and the slip increased only at one measurement point during the following 18 hours. The measurements were stopped as the changes became neglicible.

The specimen was loaded after a week when the average compressive strength of concrete was 42.7 N/mm^2. The load was increased five times in a range of working loads and then increased

to failure. The first crack appeared at the middle support at the load which was lightly greater than the calculated value of the load causing the cracking moment. Only one visible crack formed at the middle support because there was no additional reinforcement. This lead to an redistribution of the support moment so that the support reactions at the ends of the specimen were greater than calculated for a continuous slab. The deflections of the specimen increased inlinearly especially after the cracking had began in the spans. The cracking was strongly distributed along the spans with distances about 150 - 200 mm from each other in the middle.

The failure of the specimen took place in the middle of the other span as the concrete crushed due to compression. The deflections were about 250 mm in each span at failure state. The slips due to loading between the steel sheet and concrete were recorded at the ends of the specimen and they were between 0 and 0,007 mm at the failure state. The sagging moment caused by the line loads and self-weight was greater than the calculated flexural resistance of the specimen taking the steel sheet into account.

7 Design of a composite slab with unbonded tendons

Design principles were developed based on the theoretical and experimental research on steel-concrete composite slabs with unbonded tendons. A composite slab with horizontal shear resistance of the joint high enough to withstand the shear induced during the post-tensioning work can be analyzed using the principles developed for post-tensioned concrete slabs in addition that horizontal shear should be checked as a possible failure state. The effect of the anchorage force on the joint should be studied experimentally for each type of composite slab. The steel sheet can be fully utilised in the calculations of the effective stiffness and the flexural resistance of the composite slab.

References

1 CEB. CEB-FIP Model Code 1990. Vienna, Comite Europeen du Beton, July 1991. Bulletin d'Information No203, 204, 205.

2 Lin, T.Y. & Burns, N.H. Design of prestressed concrete structures, 3rd edition. Singapore 1982. John Wiley & Sons. 646 p.

3 Malaska M. & Pajari M. Long-term behaviour of composite slabs prestressed with unbonded tendons. Espoo 1996, Technical Research Centre of Finland. VTT Research Notes 1778. 29 p. + 11 App.

Composite Decking Unit of Thin-Walled Z Purlins and Thin Concrete Slab

Matti V. LESKELÄ
PhD, Civil Eng.
University of Oulu
Oulu, Finland

Matti Leskelä, born 1945, received his PhD in 1986 and has been carrying out research into composite structures from the early 1980's. His latest work has concerned problems of partial interaction and various shear connections in composite structures such as slim floors, Composite slabs and concrete filled steel tubes.

Summary

A prefabricated composite decking unit is described, in which Z and Sigma purlins are used as floor beams and are connected to a relatively shallow concrete slab. The concrete slab is cast on thin-gauge profiled sheet shuttering connected to the purlins by self-tapping and self-drilling screws in troughs in the sheeting. The behaviour of a typical decking unit and the properties of the screws as shear connectors are explained as observed in tests and in numerical analyses performed using layered beam elements.

1. Introduction

Prefabricated decking units composed of a thin concrete slab cast on thin-gauge profiled sheeting and Z and Sigma purlins represent a new development that has also been used to some extent in Finland. Their behaviour as composite structures and the behaviour of the self-tapping and self-drilling screws as shear connectors are discussed in this paper. Eurocode 4 (ENV 1994-1-1) can be applied to the design of these structures, and the validity of the design principles given in the Eurocode was verified by finite element calculation (method based on layered beam elements = LBE).

1.1 Principle of the decking unit

The load-bearing components of the unit are shown in Fig. 1. Concrete is cast on an assembly of steel components consisting of Z and Sigma purlins tied together by transverse low-profile steel sheeting and self-drilling and self-tapping screws, which also serve as shear connectors between the purlins and the concrete. It has been shown by tests that screws placed in troughs in the sheeting have enough strength and slip capacity to validate the use of partial and full shear connection designs according to the ENV-Eurocode 4 (ENV 1994-1-1 [1]). The size of the concrete cross-section is large enough to ensure of that the whole depth of the purlins is in tension or only slightly in compression so that no reduction has to be made due to instability and the simple theory of plasticity can be employed to evaluate the bending resistance according to Eurocode 4. For the resistance of self-tapping screws and similar devices, failure modes with respect to shank failure, ripping of steel, i.e. in the shuttering or the purlins, and failure of the concrete in the troughs should be considered. According to push-out tests, the resistance formula in ENV 1994-1-1, given as a function of the strength of the concrete is the most suitable for evaluating the strength of the screw connector.

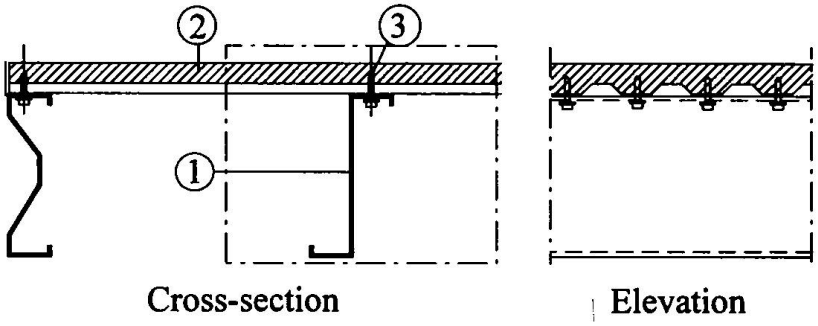

Fig. 1 Principle of the decking (showing structural components only): (1) purlins with a minimum thickness of 1.5 mm spaced at 600 mm, (2) concrete deck with a minimum thickness of 35 mm above the ribs (total depth 50 mm) and (3) screws as shear connectors.

2. Design properties

2.1 Properties of the screw connectors

The failure modes to be considered include (1) shank failure of the connector, (2) failure of the steel in the purlin flange, and (3) concrete failure in the trough. These can be evaluated according to Eurocodes 3 and 4 [1, 2]:

$$(1)\ F_{v.Rd} = \frac{0.6 A_{v.sh} f_{ub}}{\gamma_{Mb}} \quad (2)\ F_{b.Rd} = \frac{2.5 \alpha f_u d t}{\gamma_{Mb}} \quad (3)\ P_{l.Rd} = 25 \alpha \frac{A_v}{\gamma_v} \sqrt{f_{cube}(f_{cube} + 10)^{1/3}}$$

where d is the shank diameter of the screw, t the wall thickness of the purlin, f_{ub} the ultimate strength of the screw material and f_u the ultimate strength of the purlin material. Equations (1) and (2) are found in Eurocode 3, and equation (3) is a transformation from equation 6.14 of Eurocode 4. $A_{v.sh}$ is the shank area and A_v is an area calculated according to the stress diameter of the threaded section in the screw, and α may be taken as unity according to tests.

Since there is no way to evaluate the slip capacity of the connector theoretically, push-out tests according to section 10.2 of Eurocode 4 were carried out (Fig. 3). Two types of the screw described in Fig. 2 were tried, but there were no major differences in behaviour between them when the appropriate load-slip curves were considered in coordinates scaled to unity.

It was found out for the screws employed that only equations (2) and (3) should be considered, as no signs of shearing were observed in the shanks of the screws after the tests and the failure mode included both yield in bearing and failure of the concrete. In fact, (2) and (3) yield values of the same magnitude, when the grade of the concrete is at least C30/35. Equation (2) gave a slightly higher nominal resistance for the screw than (3), and it is thus recommended that equation (3) should be employed with respect to purlin materials not worse than S320 (f_{yp} = 320 MPa, f_{up} = 420 MPa).

For screws with a shank diameter of 5 mm (stress diameter 5.5 mm), the typical characteristic resistance from equation (3) varies between 6 and 7 kN, values which were exceeded by more than 10 % in the tests. The load-slip curves in the tests also showed that there is a large slip capacity for the resistance described above.

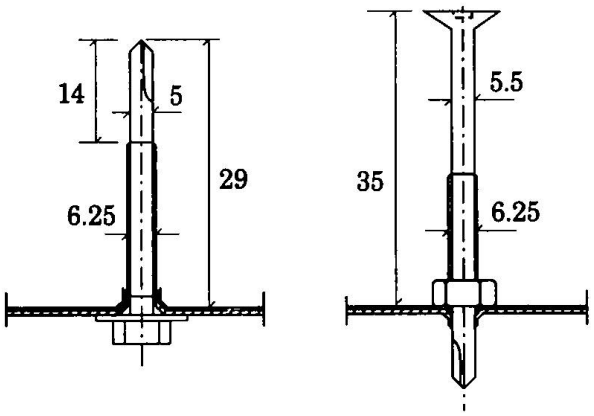

Fig. 2 Types of screws for which push-out tests were carried out. The screw on the right was used as a shear connector in the decking units tested for bending.

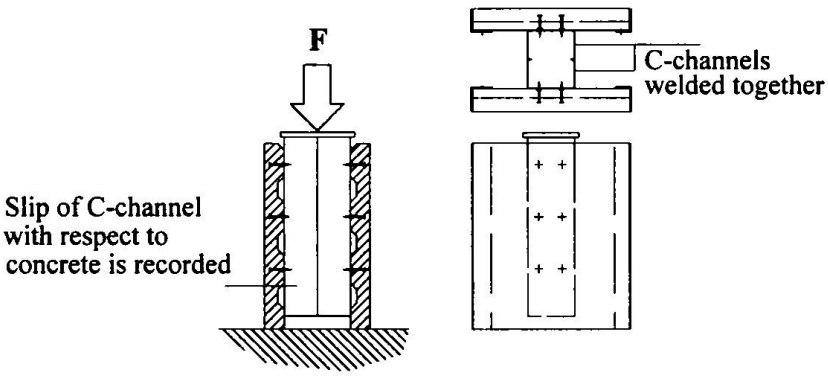

Fig. 3 Principle of the push-out test carried out to determine the load-slip properties of the screws as shear connectors. The thickness and material properties of the C profiles should be compatible with those of the Z purlins.

2.2 Composite cross-section

The span of the decking unit is always such that the whole width of the unit can be exploited for the effective concrete section. Assuming a full shear connection, a maximum value for the bending resistance is obtained. The stress state of the steel sections can be checked easily by applying the maximum design forces of the composite cross-section:

F_{tf} = maximum tensile force of the steel sections = $A_a f_{yp}/\gamma_a$
F_{cf} = maximum compressive force of the concrete section = $0.85 A_c f_{ck}/\gamma_c$

where A_a and $A_c = b_c h_{c1}$ are the total cross-sectional areas of the steel and concrete sections, respectively. Denoting that $\beta_x = x/h_{c1} = A_a f_{yp} \gamma_c/(0.85 A_c f_{ck} \gamma_a) \leq 1$ as the relative depth of the concrete section in compression, it may be easily seen that, for the purlins normally employed, $\beta_x < 1$ and the total steel section is in tension. The lever arm, z, for the evaluation of the bending resistance is $z = h_a/2 + h_{c2} + (1 - 0.5\beta_x)h_{c1}$ and $M_{pl,Rd} = zF_{tf}$. To obtain the maximum resistance, the number of shear connectors in the half span of the decking should be $N \geq N_f = F_{tf}/P_{l,Rd}$. Considering the partial safety factor for the

shear connection, γ_v = 1.25, and the length of the span in the decking unit, this cannot normally be achieved, but the degree of the shear connection, $\eta = N/N_f$, is not far from unity.

2.3 Flexural loading tests for the decking units

Three test units consisting of three 200 mm deep Z purlins and a concrete slab with a width of 1500 mm were loaded in flexure with four equal line loads across the decking at the L/5 points on the span. The load-deflection curves for the specimens are shown in Fig. 4, together with the curve calculated by the method of finite elements (LBE) developed for the purpose [3, 4]. The load-slip properties for the shear connection were adopted from the push-out tests for the screw connectors and the stress-strain curve for the cold-worked steel in the purlins was modelled based on the coupon tests.

The test loadings were continued as far as possible so as to be sure that the full plastic resistance of the composite cross-section would be obtained. A stress diagram at the termination of loading, as defined from the strain measurements and material tests, is shown in Fig. 5, and the bending moment as integrated from the stress diagram complies with the maximum moment obtained, which is greater than the resistance $M_{pl.Rk}$ calculated according to simple plastic theory and stress blocks as in Eurocode 4.

It is seen in Fig. 5 that although not the whole of the steel section is plastic, $M_{pl.Rk}$ could still be reached, due to the lever arm of the internal forces being greater than $h_a/2$. The real distribution of stresses and their resulting force may even have a beneficial effect on the total force of the connection, i.e. a fully plastic shear connection is not required in reality to balance the tensile force of the steel section, and a considerable amount of the slip capacity is left in reserve.

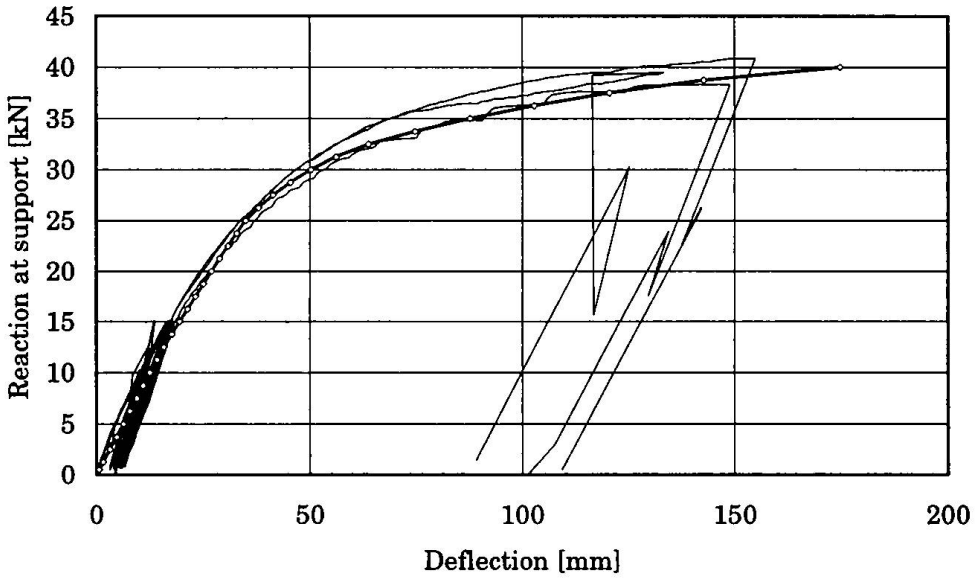

Fig. 4 Load-deflection behaviour of a decking unit having a span of 6 m, as observed in three loading tests (curves without markers) and a finite element calculation (curve with markers).

End slips were not measured in the flexural tests, but as monitored visually, they were in excess of 3 mm at the termination of loading. This would imply that the connector resistances were reached at least at the ends of the spans.

The loading in all the tests of Fig. 4 was terminated while the load could still be increased, once $M_{pl.Rk}$ had been reached. This was done due to the instability of the loading system caused by the excessive deflection.

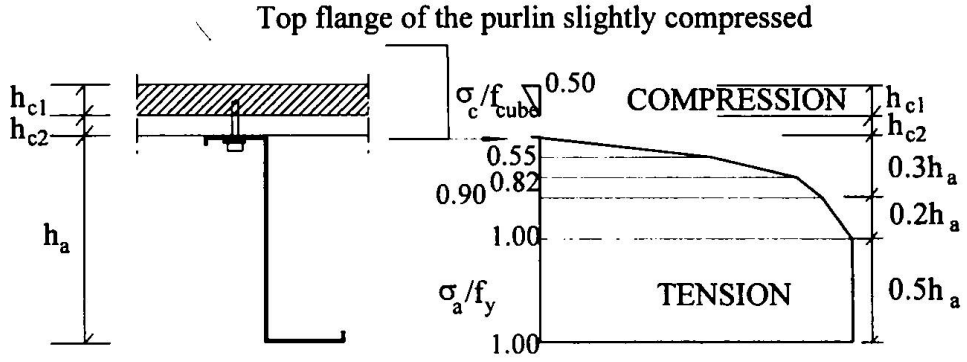

Fig. 5 Stress diagram at the termination of loading, as defined from the strain measurements.

2.4 Serviceability properties

The variation in the properties of the shear connection does not normally have any noticeable influence on the deflections in a composite beam, all the time the degree of the shear connection is close to unity. Unfortunately this is not true for the structure considered here, and the flexibility of the connection should be allowed for when evaluating the effective stiffness of the system. This may be done by increasing the nominal modular ratio, $n = E_a/E_c$, and $n_{eff} = 3n$ would be an appropriate selection for the test specimens and for considering the short-term behaviour. Even then the behaviour of the decking is satisfactory and no major design problems would occur.

To avoid discomfort due to vibration, the value of the lowest eigenfrequency, f, should be checked and should not be less than 4 Hz:

$$f = 500\pi \sqrt{\frac{E_a I_1}{mL^4}} \geq 4 \text{ Hz} \qquad (4)$$

where E_aI_1 is the effective short-term bending stiffness of the system in MNm^2, L the span of the decking in metres and m the dead-weight of the decking in kg/m. For spans not greater than 6 m the above limit is easily exceeded, and the typical eigenfrequencies then are in excess of 6 Hz. The frequency requirement in equation (4) is not presented in Eurocode 4 and not even in Eurocode 3, but only in Eurocode 5 for timber structures. However, it is equally important to consider vibrations in composite structures.

3. Discussion

The decking unit described in this paper can be designed satisfactorily by following the methods of Eurocode 4. It is shown that the shear connection provided by the self-tapping and self-drilling screws may be considered ductile, and the normal degrees of the shear connection are not much below a full connection. The resistance of the screw connectors can be evaluated conservatively according to the formulae for headed studs in Eurocode 4, employing the stress area as the effective cross-sectional area of the connector. The strength of the screw material is such that no failures in the screws are to be expected and failure in the push-out tests took the form of simultaneous yielding in bearing of the steel and shearing in the concrete.

While the resistances for bending and vertical shear, and for longitudinal shear, will not normally cause any poblems, more attention should be paid to verification of the serviceability of the system. The additional deflection due to the flexibility of the connection can be considered by an application of the increased modular ratio, which should further be increased to allow for long-term effects. The decking may be precambered in connection with the concreting, by supporting the purlins as cantilevers. The effects of concrete shrinkage during drying and solidification of the slab concrete was monitored within the flexural test specimens, and no reduction in the precamber produced by the weight of the concrete was observed during the curing period.

Detailing of the system components is not discussed in this paper, but it should be pointed out that the normal problems emerging in thin-walled structures, such as web crippling at supports, need to be remembered. They can be considered by applying the rules of Eurocode 3.

4. Acknowledgements

The kind permission of Rautaruukki to publish material related to the tests discussed is gratefully acknowledged.

5. References

[1] Eurocode 4: ENV 1994-1-1, Design of composite steel and concrete structures, Part 1.1, General rules and rules for buildings. CEN 1992

[2] Eurocode 3: ENV 1993-1-1, Design of steel structures, Part 1.1, General rules and rules for buildings. CEN 1992

[3] Leskelä, M., Calculation Models for Concrete-Steel Composite Beams, Considering Partial Interaction. Acta Universitatis Ouluensis, Series C, Technica No 16. University of Oulu, Oulu 1986

[4] Leskelä, M.V., A finite beam element for layered structures and its use when analysing steel-concrete composite flexural members. Constructional Steel Design. World Developments (354-358). Elsevier Applied Science, London and New York 1992

Design of Continuous Lightweight Structural Sandwich Panels

Paavo HASSINEN
MSc. Tech.
Helsinki University of Technology
Espoo, Finland

Lassi MARTIKAINEN
Lic. Tech.
Helsinki University of Technology
Espoo, Finland

Summary

Lightweight sandwich panels are composite structures made of two strong, stiff face layers, which are separated by a soft, thick and well-insulating core. In addition to the mechanical properties and dimensions, the static behaviour and load-bearing capacity of sandwich panels is influenced also by the flexibility of the fastening system and the support structure. The paper studies the response and strength of sandwich panels loaded by temperature difference between the face layers. It is proposed to model the flexibility of the fastenings by a simple spring model.

1. Introduction

Lightweight sandwich panels with metal-sheet faces and a plastic foam or mineral wool core are used to cover walls and roofs of industrial buildings, stores and cold stores, but also walls of office and even residential buildings. Design principles and calculation models of single-span sandwich panels are known and they have been applied without problems for years. Design of multi-span sandwich panels is a more complicated task, because continuous panels are loaded by transverse support reactions and high bending moments simultaneously at intermediate supports. Lightweight sandwich panels have high stiffness and resistance against bending moments and axial forces but they do not stand very well local transverse loads like support reactions.

Two different design cases can be distinguished at the intermediate supports. Positive support reaction is defined as resulting in compressive contact stresses in the joint between the support structure and the panel, and it is caused by wind pressure and snow load and by winter temperature difference between the faces of the panel. Positive support reaction results in local damages in the face which is placed against the support structure and which most often is the visible internal face. The second design case, negative support reaction, is defined as causing tensile forces in fasteners which fix the panel to the support structure. Negative support reaction is caused by wind suction load and summer temperature difference between the faces, and it results in local damage at the points of fasteners in the external face of the panel leading finally to the collapse of the cross-section at the support and giving rise to risks for the air- and water-tightness of the panel. After the local failures at intermediate supports, multi-span panels are in most cases able to carry significantly more load until the ultimate limit state failure of the panel.

Temperatures of dark-coloured external faces may reach a value of 80 °C in summer. In winter temperatures of -20 °C in Central Europe and -40 °C in the Nordic countries are not unusual. Thus, even the daily temperature difference between the internal and external faces may be 60 °C. In wall panels of cold stores the temperature difference in summer is even higher. Stresses caused by the temperature difference depend essentially on the shear rigidity of the core and on the flexibility of the fasteners and supports. In plastic foam core sandwich panels the shear creep of the core layer also affects the stresses and displacements caused by long-term temperature loads.

Rock-wool is a relatively new core material of sandwich panels. In addition to the usual sandwich panel applications, rock-wool core panels are applied to buildings with high requirements for fire safety. To understand the real behaviour of the rock-wool core sandwich structures, loading tests with temperature differences and mechanical loads with full-scale multi-span sandwich panels were carried through in a research project at Helsinki University of Technology. Results of the tests and analyses can also be utilized in the design of plastic foam core sandwich panels.

2. Theoretical background

Metal-sheet faces of rock-wool core sandwich panels are typically flat including only small cold-formed stiffeners for architectural aspects, in which case the theory of thin-faced sandwich beams can be applied in the analysis of the global bending moments, shear forces and deflections. The small flexural rigidity of the flat faces has effects on the local stresses and deformations close to the supports and fasteners. For the evaluation of the global stress resultants and deflections, analytical solutions have been published in several textbooks / *Stamm & Witte 1974*/. The more complicated continuous multi-span sandwich beams with flexible fastenings and supports can most conveniently be analysed using numerical methods like the finite element method.

Static behaviour of a sandwich beam fixed with flexible fastenings can be described by a finite element model consisting of a beam element, the nodal point i of which is supported against the uplift forces by a spring with a constant spring coefficient (k). The equation for the shear-flexible beam element with two nodal points (i,j) describing the beam-type sandwich structure can be written as

$$\frac{2B_s}{L^3(1+4\beta)}\begin{bmatrix} 6+k & 3L & -6 & 3L \\ 3L & 2L^2(1+\beta) & -3L & L^2(1-2\beta) \\ -6 & -3L & 6 & -3L \\ 3L & L^2(1-2\beta) & -3L & 2L^2(1+\beta) \end{bmatrix}\begin{bmatrix} w_i \\ w_i' - \gamma_i \\ w_j \\ w_j' - \gamma_j \end{bmatrix} = \frac{qL}{12}\begin{bmatrix} 6 \\ L \\ 6 \\ -L \end{bmatrix} + B_s\theta\begin{bmatrix} 0 \\ 1 \\ 0 \\ -1 \end{bmatrix} \qquad (1)$$

where B_s is flexural rigidity and S shear rigidity of the cross-section of sandwich panel, L length of beam element between the nodal points, $\beta = 3B_s/SL^2$, k spring coefficient describing the tensile stiffness of fastening, q uniform load, $\theta = \alpha_T (T_2 - T_1)/e$, α_T coefficient for thermal expansion of face material, e distance between the centroids of the face layers and T_1 and T_2 temperatures of the external and internal faces. w and γ are deflection and shear strain. $w_i' = dw_i/dx$.

Tensile stiffness of the fastening against the uplift loads has to be determined by testing. If the core material properties do not change with the outside temperature, the analysis can be based on the modulus and strength values determined in tests at room temperature. Modulae of elasticity of plastic foams decrease at high temperatures. However, the reduction at 50...80 °C is small and so the analysis with temperature-independent parameters gives acceptable approximate results.

3. Experimental and calculated results

In the project, loading tests were made with positive and negative support reactions caused by the temperature difference between the faces of test panels. In positive support reaction tests, a relatively large support width of 200 mm was used. Test panels in negative support reaction tests were fixed with two different kinds of fastenings: screws drilled through the panel to the support and special roof panel fixtures placed in the longitudinal joints between two panels (Fig. 1) / *Martikainen & Hassinen 1996*/. In this paper some test results are shown to characterize the stress resultants and deflections caused by the positive and negative support reactions and the different fastening systems (Figs. 2 and 3). Two-span test panels had equal spans of L + L = 2450 + 2450 mm. In the project, tests with other two-span panels and tests with three-span panels were also made, the results of which indicated the same conclusions as reported in this paper.

The external face of the full-scale test panels was heated by infra-red heaters, while the temperature of the internal face was kept at a room temperature of 20 °C. The core of the test panels consisted of structural rock-wool, in which the fibres run normal to the faces of the panel. The flat faces were made of steel sheet with steel thicknesses of 0.48 and 0.46 mm in the exterior and interior faces, respectively. Total depth and width of the panels were 100 mm and 1200 mm, respectively.

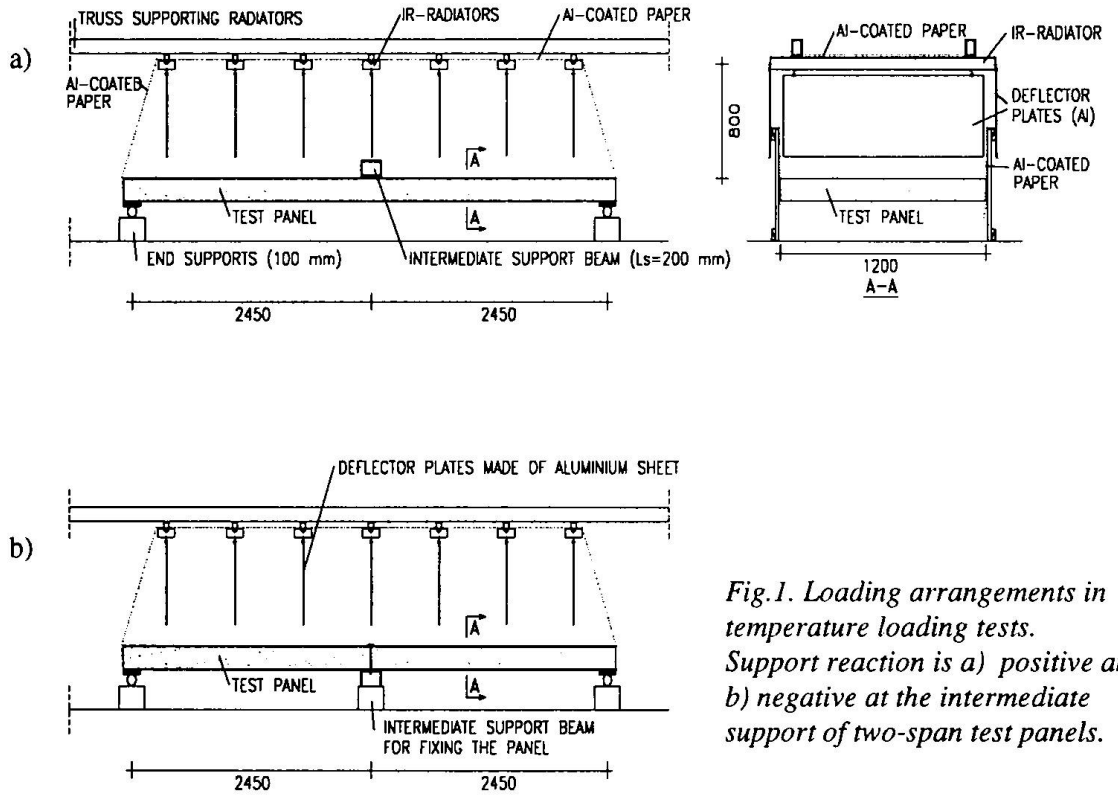

Fig.1. Loading arrangements in temperature loading tests. Support reaction is a) positive and b) negative at the intermediate support of two-span test panels.

Experimental results have been compared with calculated results using the linear theory of elasticity and by taking into account the shear deformations of the core layer and the tensile flexibility of the fastening (1). Shear deformations of the core result in app. 20% of the total deflection of the test panel and, therefore, are of high importance in the analysis of test results.

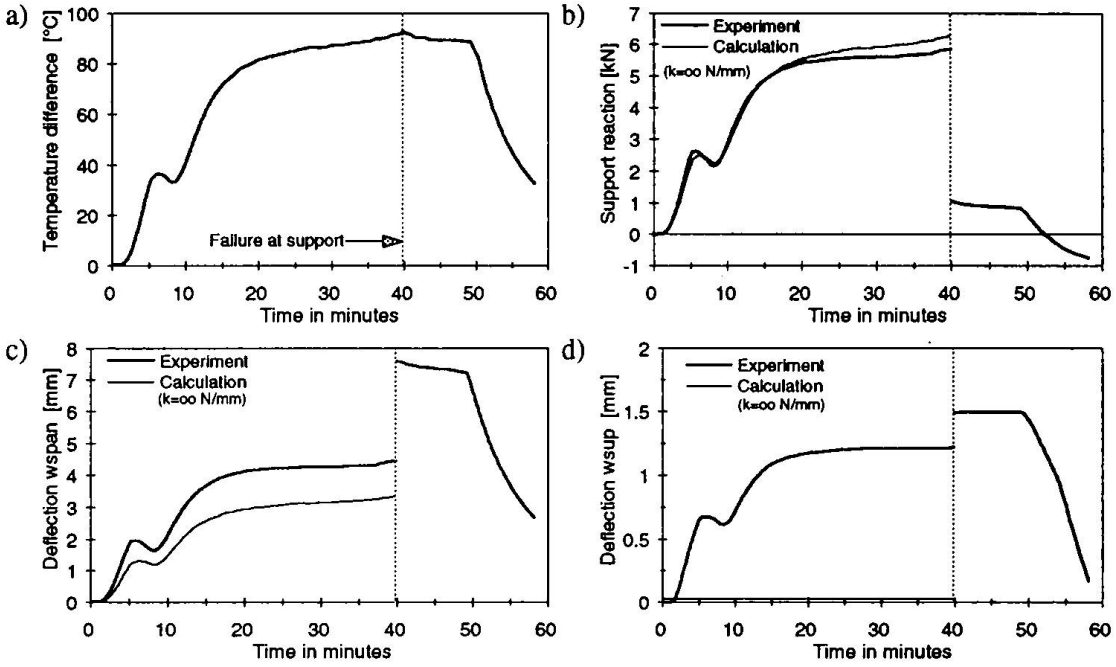

Fig. 2. Experimental and calculated ($k = \infty$) results of two-span test panel loaded by temperature difference in positive support reaction test. a) Temperature difference between the exterior and interior face, b) central support reaction, c) mid-span deflection and d) vertical displacement between the panel and the support structure at the central support. Dotted line shows the time point of local failure in the compressed external face at the central support.

In positive support reaction tests, the test panel is pressed against the support beam. The transverse flexibility at the intermediate support is caused only by the local compressive and shear deformations in the core close to the intermediate support. Calculated support reaction is slightly higher and the mid-span deflection smaller than the corresponding experimental values, if the spring constant k describing the stiffness of the support in the calculations is assumed to be infinite $k = \infty$ (Fig. 2). In current design calculations the supports are modeled to be completely rigid, which seems to be a valid assumption in the loading case of positive support reaction */ CIB 1993/.*

If the central support reaction is negative, the transverse flexibility is caused by the deformations of the fasteners and the local deformations in the core and exterior face close to the fasteners. Additional flexibility in sandwich panels fixed with roof panel fixtures is caused by the transverse curvature of the panel between the longitudinal joints. The transverse curvature results in a transverse tensile stress field in the exterior face, which further stiffens the compressed exterior face against the local buckling failure. The test panel fastened with roof panel fixtures did not fail in the test, which is due to the high flexibility of fastening and the transverse curvature of the compressed exterior face. The compressed face of the test panel fixed to the support structure with four screws failed locally at a temperature difference of app. 61°C (Fig. 3).

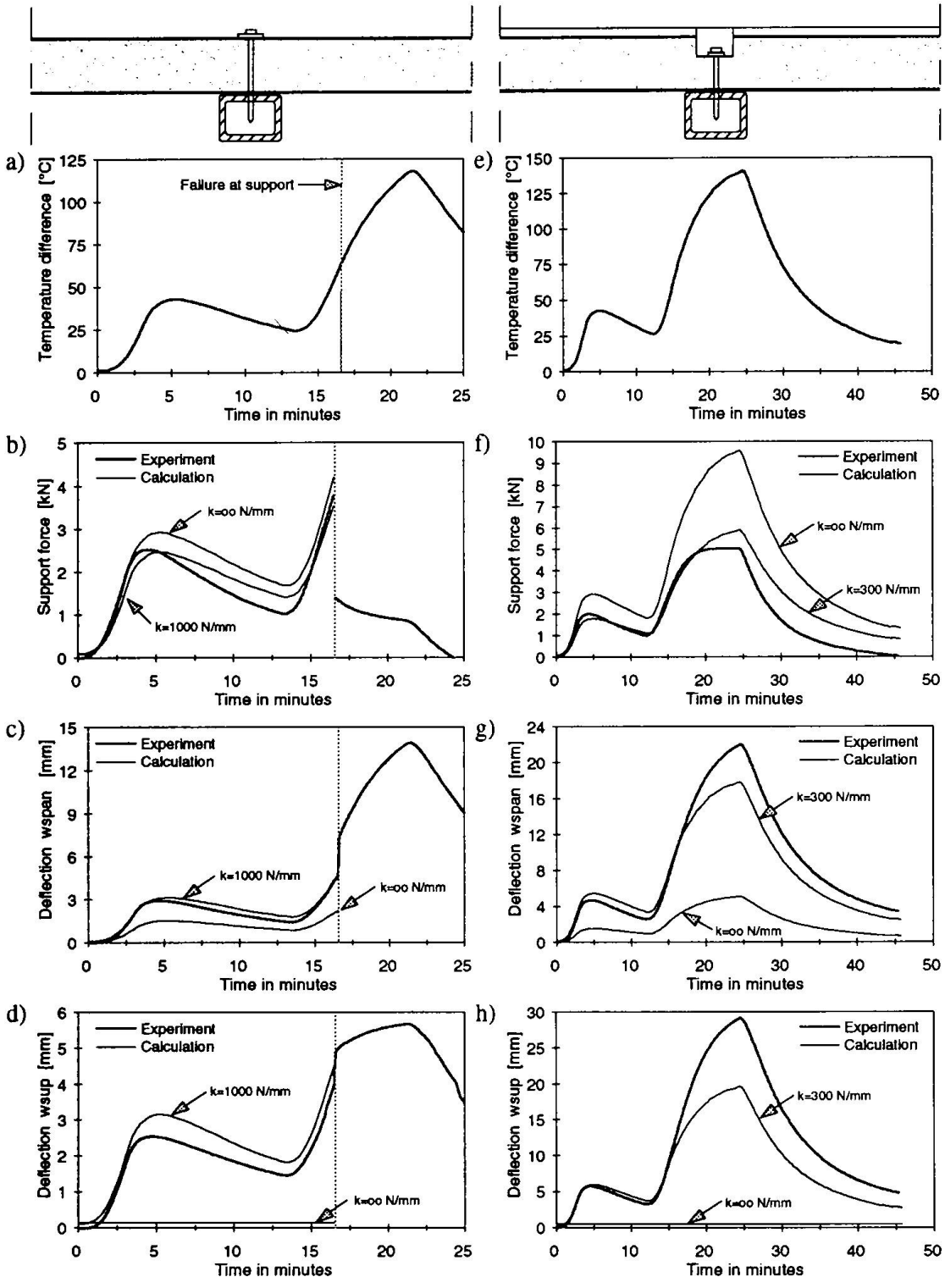

Fig. 3. Experimental and calculated results of two-span test panel loaded by temperature difference in negative support reaction tests. At the central support the test panels are fixed with four screws drilled through the panel (a...d) or with two roof panel fixtures (e...h).
a & e) Temperature difference between the exterior and interior face, b & f) central support reaction, c & g) mid-span deflection and d & h) vertical displacement between the panel and the support structure on central support. Dotted line shows the time of local failure.

The calculation model based on rigid supports, k =∞, overestimates the support reactions in negative support reaction tests and thus, also the stresses caused by the temperature difference. The model underestimates strongly the mid-span deflections and, naturally, does not show the vertical displacements between the panel and the intermediate support (Fig. 3). If the finite spring coefficients, k = 1000 N/mm and k = 300 N/mm, describing the tensile stiffness of the screw fastening and the roof panel fixture are added to the calculation model, the calculated results are in reasonable agreement with the experimental results.

4. Summary and Conclusions

Temperature differences result in large bending moments at intermediate supports of continuous multi-span sandwich panels. At intermediate supports the bending resistance is reduced because of the transverse support reaction. The reduction depends on the direction of the support reaction, i.e., support reaction is positive or negative, and further, on the support width and the type and number of fasteners. Unfortunately, the space in this paper does not allow further details concerning the resistances of sandwich panels. In practical design work, bending resistance of the cross-sections at intermediate supports is assumed to be 80-90 % of the bending resistance in the spans. An accurate evaluation of stresses caused by the temperature differences but also a careful analysis of the bending resistances and support reaction resistances are important in order to achieve economical design and use of lightweight sandwich panels. Both sides, i.e., the stress and resistance sides, of the design equation are of equal consequence in design.

In the current design calculations, the supports are assumed to be completely rigid. The model is valid, if the panel is pressed against the support structure and the support structure is relatively rigid against the transverse loads. But if the panel is loaded by wind suction loads or summer temperature differences causing tensile forces in fasteners, the finite flexibility of the fastenings should be taken into account. In most loading cases, the support can be modelled by a simple spring having a constant spring coefficient. A bilinear spring is needed for the loading cases in which the direction of the support reaction may change from positive to negative and vice versa.

Acknowledgements

The research is financially supported by the Technology Development Centre and Paroc Oy Ab. The support is gratefully acknowledged.

References

European Convention for Constructional Steelwork (ECCS) & International Council for Building Research, Studies and Documentation (CIB). 1993. Preliminary European Recommendations for Sandwich Panels with Additional Recommendations for Panels with Mineral Wool Core Material. CIB Report, Publication 148. 142 s.

Martikainen, L. & Hassinen, P. 1996, Load-bearing capacity of continuous sandwich panels. Helsinki University of Technology, Department of Structural Engineering, Report 135. 178 p. + app. 43 p.

Stamm, K. & Witte, H. 1974, Sandwichkonstruktionen (Sandwich structures). Springer-Verlag. 337 p. (in German).

Slimdek - Development of an integrated Floor System

Peter J. WRIGHT
Manager Struct. Syst. Dev.
British Steel
Redcar, UK

Peter Wright, BA. C.Eng. MIStructE AMICE born 1950, worked for many years with consulting Engineers in London on a variety of major structures before joining the British Steel. He managed the Structural Advisory Service from 1989 and has been responsible for the development of the Slimdek system.

Summary

The paper outlines the Slimdek floor system introduced in 1997, which allows the integration of the strucural and service elements in multi storey building construction. The system eliminates downstand steel beams and introduces new beam and deck components designed to maximise structural efficiency.

1. Overview

In the United Kingdom, Ireland and Sweden, steel frames have achieved a high market share through the introduction of efficient design methods of floor construction. Structural systems based on both pre-cast units and composite steel decks, supported on steel beams either below or within the floor plate have been well researched and reported. These have until now been based on standard components.
In May 1997 British Steel plc launched a totally new floor system which addressed the need to integrate the Architectural, Structural and Servicing demands of construction in a single engineered package - **Slimdek** See fig 1.

The initiative is an innovative approach to the design and construction of multi storey buildings, being engineered to optimise efficiency in both room temperature and fire design states, whilst allowing extensive options for both passive and active servicing of structures. The project has built on the experiences of the Slimflor sections developed for the UK construction market.

In 1991 British Steel invested heavily in its Lackenby Beam mill at Teesside which gave the capability to roll the first new Universal Beam section for over forty years, the Asymmetric Slimflor Beam (ASB). Coupled with this new beam is the design and production of a new deep composite profiled steel deck, SD225. These products, together with a new Rectangular Hollow Slimflor Beam (RHSFB) and the existing Slimflor Beam SFB) form the major components of **Slimdek.**

The **Slimdek** system development has been managed by the Structural Systems Development Team of British Steel SP&CS. The project has been a joint initiative based on team work between several British Steel Divisions, The Steel Construction Institute and the UK Department of Trade and Industry through the LINK Enhanced Engineering Materials Programme.

2.1 The Asymmetric Slimflor Beam (ASB)

The Asymmetric Slimflor Beam (ASB) is designed for with maximum standardisation and optimum structural efficiency in both the normal design state and at elevated temperatures.
The section is rolled with an embossed top flange to enhances the shear bond between the beam and the over-lying in-situ concrete thus eliminating the need for welded shear connectors. Tests have shown that a design shear bond strength of $0.6N/mm^2$ can be developed between the steel and concrete.

As with the existing Slimflor Fabricated Beam (SFB) the ASB achieves a fire rating of 60 minutes due to the inherent fire resistance of the section. It has a web of greater thickness than that of the flange to achieve the fire resistance properties. The thicker web also enhances the section's torsional properties. Three ASB sections are currently available, two of which are nominally 280mm deep and one 300mm deep. These dimensions have been chosen to achieve specific target load and span characteristics. The load / span range is targeted for the medium span building :

Beam Section	Beam Span	Deck Span	Imposed Load kN/m^2
280ASB 100	6m	6m	5 + 1
280ASB 136	7.5	6	3.5 + 1
	6	7.5 propped	5 + 1
300 ASB 153	7.5	7.5 propped	3.5 + 1
	7.5	6	5 + 1

The ASB is designed specifically for use with the SD225 composite deck and has been designed to enhance the deck's capabilities by allowing service voids to be formed through the web at 600mm centres, aligned with the deck profile.

2.2. The SD225 Deck

This advanced composite deck profile is 225mm deep with spanning capabilities of up to 6.5m unpropped and up to 9m propped. Composite action is improved by the transverse embossments in the deep deck profile, and by reinforcing bars located in the ribs of the deck. These bars also enhance the fire resistance of the slab. The deck has been detailed to facilitate complete service integration either within the depth of the deck profile and through holes in the ASB section, or hung from a dovetail housing in the rib trough.
'Cut outs' are provided at the ends of the deck sheet to facilitate ease of handling on site and also to ensure adequate placement of concrete around the steel section. The SD225 decking is supplied by Precision Metal Forming Ltd., a subsidiary of British Steel.

2.3. RHSFB Section

In order to achieve a completely flat slab finish, the RHSFB has been developed to complement the **Slimdek** system. It consists of a Rectangular Hollow Section with a plate welded to its underside. The hollow section has superior torsion properties to normal open sections and is ideal for use as an edge beam where the outer face of the RHS is often exposed giving the ability to fix cladding attachments directly on to the steel section.

3. Advantages of Slimdek

The System is fully engineered for minimum construction depth with all the benefits Slimflor plus:

- **Composite Action without the need for shear stud connectors**
  The ASB section is rolled with a patterned top flange to enhance the composite action with the in-situ concrete, so eliminating the use of shear connectors. This major advantage has been validated through extensive testing.
  The dynamic and static load tests carried out at City University on 7.5m span ASB sections have demonstrated that a design shear bond strength of 0.6N/mm^2 may be developed around the upper flange and web. This composite action is enhanced by the raised pattern on the top flange. However, it is not normally necessary to utilise full composite action at the ultimate limit state, since serviceability and fire limit states tend to control the design.

- **Inherent fire resistance**
  The ASB gives optimum design performance in both the normal design state and at elevated temperatures. The section has a web of greater thickness than that of the flange which not only provides good fire resistance properties but, enhances the section's torsional properties. The three current ASB sections have been developed to achieve 60 minutes fire resistance in **Slimdek** construction without requiring protection of the exposed bottom flange.

- **Savings in fabrication costs**
  By eliminating the need to fabricate up the Slimflor section, a lighter and more economic section is produced. Economic assessments of the **Slimdek** system have shown that there is a potential weight saving in the order of 15% to 25% over the conventional Slimflor concept. Lower costs for the attachment of connection plates and the avoidance of secondary beam connections are also achieved.

- **Readily available section with defined properties**
  Because the ASB is a rolled section, its properties are easily calculated and tabulated. All the sections are Class 1 to EC3, thus allowing their moment resistance to be calculated for plastic analysis principles.

- **Reduced Construction Costs**
  The spanning capability of the SD225 deck allows most short to medium span floor grids to be achieved by the system without the need for secondary beams. This allows the weight of the ASB to be offset against the costs of construction with primary and secondary beams of traditional composite decks. The savings in shear studs, fire protection and fabrication make **Slimdek** a highly competitive system.

- **Enhanced servicing of deck**
  The **Slimdek** system has been designed to allow the maximum ease of serving either below the deck or integrated into the floor system. Simple fixing systems for service supports have also been developed to compliment the system.

4. Slimdek details

4.1. ASB

Currently three ASB sections are available for use in the system. Each are designated by their nominal weight, 280 ASB 100, 280 ASB 136 and 300 ASB 153, and all are rolled in S355 grade steel. Common to all three sections is a nominal 190mm wide top flange and a nominal 300mm wide bottom flange onto which the SD225 deck spans. The required end bearing for metal decks of 75mm is thus satisfied. The optimum span range for the 280 ASB section is between 6.0m and 7.5m. The 300 ASB 153 section has greater load carrying / spanning properties and is designed so that the slab surface can be cast 30mm over the top of the section, thereby achieving composite action, or alternatively flush with the top of the section (non-compositely). For the latter condition additional bars are required to pass through the section to develop the necessary tying action in the floor slab.

The slab depth is controlled by the concrete over the top of the ASB to permit the placement of crack control mesh. 30mm is the minimum figure allowing a total depth of 290mm to 315mm, depending on the section size. These slab depths satisfy the insulation requirements for 60 minutes fire resistance with both normal and lightweight concrete. When designing beams with a concrete cover to the steel section greater than 60mm concrete above this thickness is ignored in strength and stiffness calculations.

4.2. SD225 Decking

The new deck developed for the **Slimdek** system is designated SD225. This deck has been designed to achieve greater unpropped spans than any other deck todate, and also to facilitate erection and subsequent servicing operations. The wide re-entrant profile to the crest increases the effective use of the steel, and allows the services fixing developed for the system to be easily clipped into position by hand. Additional re-entrants in the rib give additional fixing points for the ceiling grid. As with all composite decks embossments rolled into the steel along the length of the sheet generate the bond to resist slip with the concrete topping. Both normal and lightweight concretes may be specified. The minimum depth of the SD225 slab formed is 290 which permits the 30mm cover to the 280ASB.

5. Longitudinal Shear Connection

The encasement of the ASB by the concrete topping to the SD225 deck produces a block of concrete which is effectively locked between the flanges of the section. Mesh reinforcement across the top flange acts to transfer longitudinal forces from this block into the slab, and controls cracking across the beam. The degree of interaction is relative to the shape of the section, the slab depth and width, and the natural bond between steel and concrete. The ASB uses an embossed pattern to the top flange to enhance the natural bond and to permit this bond to be effectively taken into account in the design.

A test programme, designed by the Steel Construction Institute, was conducted, to establish the appropriate shear bond, and to develop a design methodology for the ASB. Dynamic tests on a load up to 85% of the bending resistance of the steel section, through 1000 cycles, and static loads to establish the unloading stiffness of the section after plasticifation started.The permanent deflection measured load test was less than 1mm, proving negligible slip between steel and concrete.
The failure criteria for the static load tests was set at span/50. This failure criteria was achieved at very close to the plastic resistance of the composite section. Back analysis of the results proved that the shear connection between steel and concrete was between 90 and 100%, and the corresponding increase in bending resistance of the plain section between 42 and 46%

From the tests a design methodology for ASB sections has been established which utilises the shear bond generated between the steel and concrete topping to three decking profile. Minimum and maximum concrete cover to the steel sections have been set to ensure the bond generated is achieved. Typical calculations are normally found to be serviceability dependent for room temperature calculations.

6. Fire Resistance

The ASB Section generates optimum design efficiency at the fire limit state. The web is more effective than the exposed bottom flange, which acts at a reduced strength in a fire situation to achieve 60 minutes fire resistance. The minimum depth of concrete over the top of the decking is dictated by fire insulation requirements at the fire limit state. Recommended depths over the top of the SD225 deck to achieve 60 minutes are 60mm for lightweight concrete and 70mm for normal weight concrete.
The fire resistance of the slab formed with SD225 deck is achieved by reinforcing bars within the deck ribs seated in circular spacers which locate the bars and ensure adequate cover.
Fire testing on the ASB with decking was carried out at the Warrington Fire Research Station, UK. The results of the tests showed that the shear bond between the ASB section and the concrete is not decreased at elevated temperatures, and the bond can be used for in design at the fire limit state. This allows the ASB sections to perform at maximum efficiency in both cold and fire design.

7. Service Integration

In buildings where, for individual comfort and control, there is a need to accommodate a variety of natural and mechanical ventilation systems, pre-planning can have a beneficial effect on the choice of structure. The **Slimdek** system gives free space directly below the floor slab, for unhindered services.

The SD225 deck allows vertical ductwork to be taken through openings formed by either wiring polystyrene blocks in place, or by using shuttering, prior to concreting. After the slab is cast and adequately cured the deck can be cut away to allow access for vertical service runs. It is also possible to integrate the services within the depth of the deck.
The SD 225 deck is detailed to allow extensive underfloor servicing. The wide indent dovetail to the top of the crest is intended for service suspension, reducing the structural floor depth by permitting services to pass through the ASB section in pre-defined duct openings.

Circular or oval shaped openings may be formed in the webs of the ASBs. For detailing purposes, the openings are located at 20mm above the top of the bottom flange of the steel section. This allows clearance for the horizontal services support hangers to be located above the duct. The openings may be up to 160mm deep and the oval shaped openings may be up to 320mm wide.
When web openings are used to integrate the services, the ASB sections will always require fire protection to be applied to the underside of the bottom flange.

8. Thermal Capacity

Thermal performance and inherent durability necessitate the use of building materials and components that can respond to external environmental conditions and provide stable interior environmental control. There is a growing demand for the construction industry to tackle the 'green issues' of energy consumption both during production / construction, and throughout the operational life of the building.

The system provides simple options for natural ventilation, night time cooling and air circulation within the profile ribs reducing reliance both on mechanical services and energy requirements.

Steel frames allow the sought after flexibility of use and adaptability for the future which are essential elements for sustainable development.

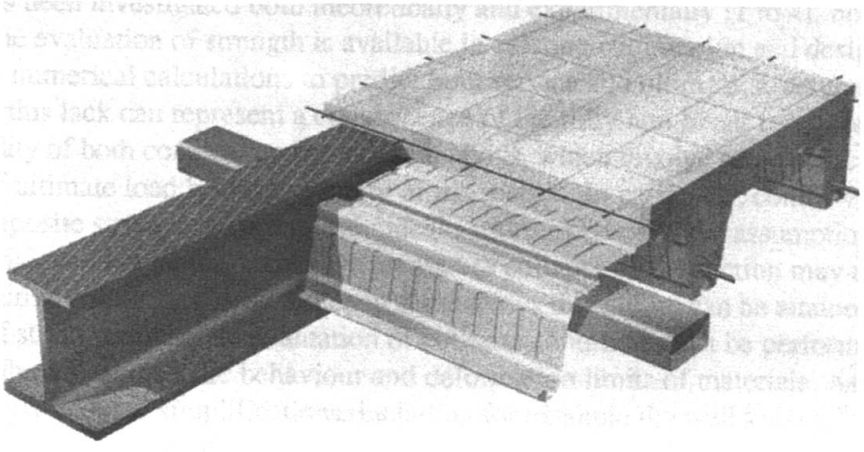

Slimdek, Slimflor, SD225 and **ComFlor** are Registered Trade Marks of British Steel plc.
A patent has been applied for on the Slimdek system.

Leere Seite
Blank page
Page vide

Plastic Design of Aluminium-Concrete Composite Sections: a Simplified Method

Alberto MANDARA
Eng.
University of Naples
Naples, Italy

Alberto Mandara, born 1963, is Research Assistant at the Second University of Naples. Graduated in 1987, he got the PhD degree in 1993. Author of more than 40 papers on steel and aluminium structures. Presently member of UNI-CIS/SC3, "Steel and Composite Structures" and UNI-CIS/SC10 "Structural Restoration" and CEN-TC 250/SC9 " Aluminium Alloy Structures".

Federico M. MAZZOLANI
Prof. Dr.
University of Naples
Naples, Italy

Federico M. Mazzolani, born 1938, is Full Professor of Structural Engineering at the University "Federico II" of Naples. Author of more than 350 papers and 12 books in the field of metal structures, seismic design and rehabilitation. Member of many national and international organisations. Presently Chairman of UNI-CIS/SC3 "Steel and Composite Structures", CNR Fire Protection", ECCS-TC13 "seismic "Design" and CEN-TC 250/SC9 "Aluminium Alloy Structures".

Summary

A practical procedure for the design of aluminium-concrete composite sections in bending is presented in this paper. The actual inelastic behaviour of materials is considered for the evaluation of section ultimate load bearing capacity. A numerical analysis has been performed for evaluating the response of aluminium alloy section, whereas the existing CEB regulations have been applied for the prediction of concrete inelastic response.

1. Foreword

Despite several applications in the field of bridge structures in France and in U.S.A., aluminium-concrete composite structures are not yet covered by specific regulations, neither in Europe, nor overseas. At the present stage of knowledge, even though the bending behaviour of such structures has been investigated both theoretically and experimentally [1 to 4], no practical method for the evaluation of strength is available in existing codification and designers must face cumbersome numerical calculations to predict both service and ultimate structural response. To some extent, this lack can represent a consequence of the fully non linear behaviour and relatively limited ductility of both concrete and aluminium alloys, which involve some difficulties in the evaluation of ultimate load bearing capacity of the section. In particular, contrary to steel-concrete composite structures, fully plastic idealizations, relying on the assumption of infinitely ductile material, can not be used, because premature collapse of the section may occur due to excess of strain in aluminium alloy. Since in some alloys this failure can be attained for relatively low values of strain, an accurate evaluation of collapse condition must be performed, by taking into account the actual inelastic behaviour and deformation limits of materials. As a consequence, some commonly adopted simplifications, including for example the well known "stress block" approach for the evaluation of concrete ultimate strength, can not be assumed.
On the basis of the existing knowledge in the field of aluminium alloys [5], a method for the prediction of the ultimate strength of composite sections in bending is presented in this paper. The procedure has been fitted on the outcoming of a well tried numerical simulation, which has shown to be in good agreement with experimental results [4]. Since the method is consistent with both CEB regulations on reinforced concrete structures and CEN Eurocode 9 on aluminium alloy structures, it could represent a first attempt to implement this topic into European regulations.

2. Limit state definition

A typical composite aluminium-concrete section is depicted in fig. 1a, where the relevant geometrical parameters are also shown. The slab width B can be the actual one or the effective one B_{eff}, depending on beam geometrical ratios and restraint conditions (see for example EC4 for the evaluation of B_{eff}). G' and G are the geometrical centroids of the aluminium beam and of the whole section, respectively.

For the evaluation of ultimate strength of the section, a preliminary definition of material laws is necessary. The material models adopted are shown in fig. 2. The well known CEB σ-ε law with a parabolic branch up to a strain of .2% and an ultimate strain of .35% is adopted for concrete in compression (fig. 2a). The tensile strength of concrete is neglected. This model has been chosen because it is widely referred to into both literature and codification on r.c. structure; in addition, it makes the evaluation of the plastic behaviour of the concrete slab quite simple, the response of rectangular r.c. section made of this material being extensively tabled in literature.

The classical elastic-plastic σ-ε law is assumed for reinforcement steel bars (fig. 2b). No strain limitation is assumed for steel, neither in tension, nor in compression. Obviously, the maximum deformation in compressed bars must comply with the maximum allowed strain for concrete.

The three-parameter non linear Ramberg-Osgood model $\varepsilon = \sigma / E + 0.002(\sigma / f_{0.2})^n$ has been assumed to interpret the behaviour of aluminium alloys (fig. 2c). In this case, owing to a strain-hardening effect, a perfectly plastic behaviour does not exist, the material response being continuously increasing for a wide range of strain. Since for some alloys the actual deformation capability may result in not very high values of strain, a conventional deformation limit must be set to define the ultimate limit state of material. According to the usually followed approach for the evaluation of ultimate strength of aluminium sections [5], if $\varepsilon_e = f_{0.2} / E$ is the deformation calculated elastically at the conventional yield point $f_{0.2}$, a maximum strain limit $\varepsilon_5 = 5\varepsilon_e$ or $\varepsilon_{10} = 10\varepsilon_e$ can be assumed, depending on the alloy ductility features. The strain limits ε_e and $\varepsilon_e + 0.002$ are also considered, as elastic limit state and conventional yielding limit state, respectively.

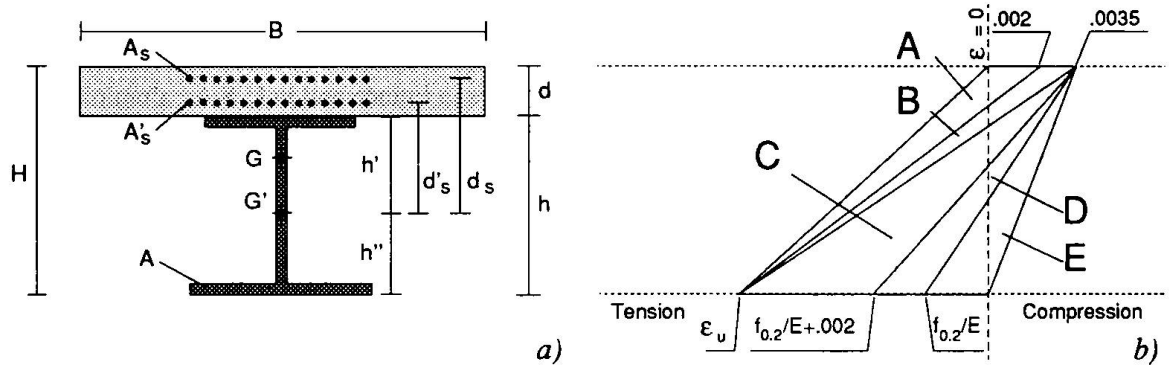

Fig. 1 Geometrical magnitudes (a) and failure conditions (b) of the composite section.

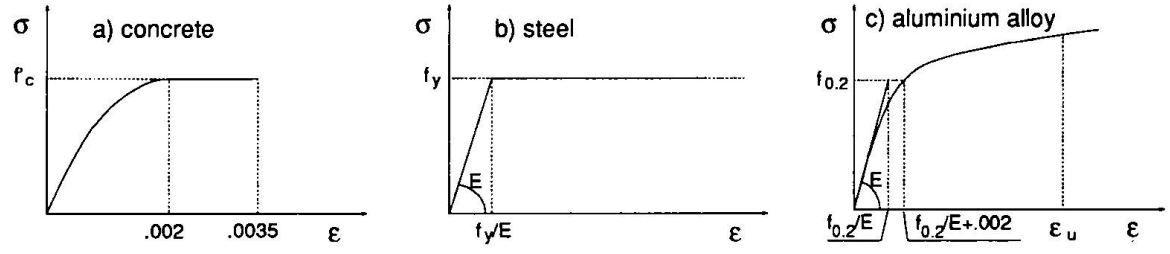

Fig. 2 Material laws

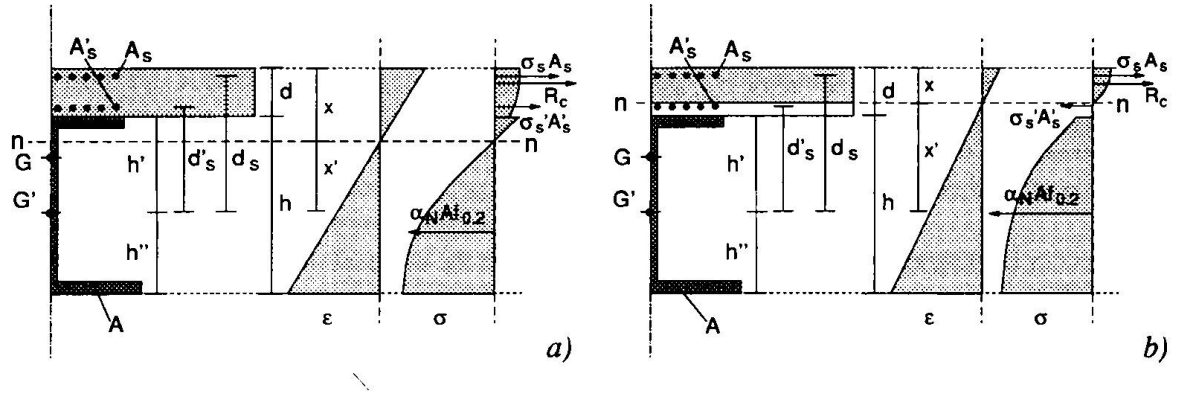

Fig. 3 Distribution of internal actions in the cross-section [a) $x > d$, b) $x < d$]

3. Evaluation of ultimate bending strength

Conventionally, it is assumed that the collapse of the section is attained when one of the components reaches the limit value of strain. This may be the aluminium beam and/or the concrete slab, depending on the geometrical and mechanical features of the section. Since generally neither concrete nor aluminium alloy exhibit very large plastic deformations at failure, scarce reliance can be put on the post-elastic strength of material in the evaluation of the plastic response of the section. For this reason, the common approach used for steel-concrete composite sections, based on indefinitely plastic behaviour of material, can not be followed. This involves that many calculation simplifications allowed by the large ductility of steel, such as for example the well known "stress block" idealisation for concrete compressive resultant force, can not be used. Also, the concept of "balanced failure", well known in the literature on r.c. structures, looses most of its meaning.

As being stated, the possible failure conditions of the section, represented in fig. 1b, are exclusively related to the attainment of the above strain limits. Since the assumption of plane cross section up to collapse is made, such conditions are represented by lines, each of which corresponds to a defined location of neutral axis *n-n* at failure (see parameters x or x' in fig. 3). This will fall within the zones marked in fig. 1b: zones A and B correspond to the failure of the aluminium alloy, represented by an ultimate strain ε_u equal to ε_5 or ε_{10}, whereas zones C, D and E represent conditions of concrete collapse by crushing. As for all bending problems, the value of x (or x') is determinated by an equilibrium condition along the longitudinal axis of the beam. According to the notation shown in fig. 3, this condition may be written in the form:

$$A_s\,\sigma_s \pm A'_s\,\sigma'_s + f'_c\,Bx\,\Psi - \alpha_N\,f_{0.2}\,A = 0 \qquad (1)$$

The terms in Eq. (1) are shown in fig. 3, in the case when $x > d$ (fig. 3a) and $x < d$ (fig. 3b). They are to be intended in absolute value. The notation "±" means that σ'_s must be taken positive when $d'_s > x'$ and negative when $d'_s < x'$. The magnitude $f'_c\,Bx\,\Psi = R_c$ is the resultant of compression force of concrete, Ψ being a nondimensional parameter which takes into account the actual non linear stress distribution in compressed concrete. The values of Ψ are a function of the neutral axis position x/d and can be found in the current literature on r.c. structures for the assumed σ-ε law in the case of rectangular section. The term α_N represents the resultant of normal stresses acting on the aluminium section (see fig. 3); it may be expressed as:

$$\alpha_N = \frac{1}{Af_{0.2}} \int_A \sigma dA \qquad (2)$$

A being the cross sectional area of aluminium beam.

For a given limit state, i.e. for a given strain limit assumed for the alloy at the more stretched fibre of the section, α_N is a function of the σ-ε law of material, of the type of cross section, represented through the geometrical shape factor α_0, as well as of the ratio x'/h.
Similarly, based on the notation of fig. 3, the rotation equilibrium is expressed by the equation:

$$M_u = A_s\sigma_s d_s \pm A'_s\sigma'_s d'_s + f'_c Bx\Psi (d + h' - \lambda x) + \alpha_M f_{0.2} W \qquad (3)$$

The terms in Eq. (3), expressed in absolute value, represent the moment of each internal action evaluated respect to the geometrical centroid of the aluminium section (see Fig. 3). For the sign of σ'_s the same consideration made for N_u holds. λ is a nondimensional parameter which considers the resultant of concrete compressive force in its actual position. As for Ψ, its values can be found in the literature on r.c. structures for the case of rectangular section as a function of x/d. The term α_M is given by the following relationship:

$$\alpha_M = \frac{1}{Wf_{0.2}} \int_A \sigma z dA \qquad (4)$$

W being the resistance modulus of the aluminium section and z the distance from its centroid.
α_M represents the nondimensional resisting moment of the aluminium section around the geometrical centroid of the double-T profile. As for α_N, α_M is a function of the strain limit assumed for the alloy, of the σ-ε law of material, of the geometrical shape factor α_0 of the section, as well as of x'/h.
For a given deformation limit at the most stretched point of the section, the values of α_N and α_M have been calculated by means of numerical analysis as a function of x'/h. In practice, a value of x'/h is set and then the section overall response in terms of axial action $\int_A \sigma dA$ and resisting moment around the centroid $\int_A \sigma z dA$ is evaluated for each relevant limit state. The values of α_N and α_M are given in Figs 4 and 5 as a function of x'/h for a I-section with geometrical shape factor $\alpha_0 = 1.1$ and for values of the hardening parameter of the Ramberg-Osgood law equal to 8, 16 and 32. Values of limit strain equal to ε_e, $\varepsilon_e + 0.002$, ε_5 and ε_{10} have been considered in order to make possible the evaluation of section response at all relevant limit states.

4. Application of the method

The application of the method is based on the evaluation of the neutral axis depth x (or x') from Eq. (1) and on the subsequent evaluation of M_u from Eq. (3). Since a direct evaluation of x' is not possible from Eq. (1), σ_s, σ'_s, Ψ and α_N being function of x', a trial-and-error procedure must be applied: a tentative value of x is assigned, then, by considering that $x + x' = H - h''$, the obtained value of x is compared with the assumed one and corrected up to obtain the same value given when starting the calculation. All the magnitudes σ_s, σ'_s, Ψ and α_N are to be calculated according to the assumed value of x. If intermediate positions of x between the defined limit states are found, α_N may be evaluated by means of linear interpolation between the curves of fig. 4. This generally occurs when the ultimate limit state of the composite section is attained due to excess of compressive strain into concrete. As a rule, in such cases the deformation at the tensioned edge of the alloy is not equal to any of the defined limit states and, consequently, linear interpolation must be made.
In order to make the calculation easier, a preliminary evaluation of the B values, corresponding to the relevant location of x'/h at the ultimate limit state, can be made. The comparison with the actual value of B will allow to know the range in which x'/h will fall at collapse for the section under consideration.

When the neutral axis position x is known, the calculation of M_u from Eq. (3) is straightforward, being all terms σ_s, σ'_s, Ψ, λ and α_M calculated as a function of x. The evaluation of α_M may be done from fig. 5, directly or by means of linear interpolation, depending on the values of x.
The calculation procedure can be generalised to evaluate the section bearing capacity even for serviceability limit states. Since all limit states are defined by a given material strain limit ε_{al} or ε_c, the corresponding values of section curvature, given by $\chi = (\varepsilon_{al} + \varepsilon_c)/H$, may be calculated. In this way, a piecewise moment-curvature relationship may be plotted for the section.
A comparison between the procedure proposed and the results of a numerical analysis is shown in Fig. 6a, where the M - χ curve is depicted for a composite section made of a double-T extruded aluminium alloy profile with H=200 mm and a 60mm thick concrete slab, reinforced with two rows of ∅10mm bars (Fig. 6b). This example could reasonably represent the case of a floor structure, having main girders spaced 1000mm. The geometrical and mechanical features are shown in Fig. 6b. All material deformation limits referred to in fig. 1b have been considered. The corresponding values of bending moment are marked on the M - χ curve. The values of α_N and α_M have been evaluated approximately assuming $n=16$. The comparison shows a quite satisfying agreement, with results coming from the simplified procedure proposed herein slightly on the safe side with respect to those provided by the more refined simulation approach.

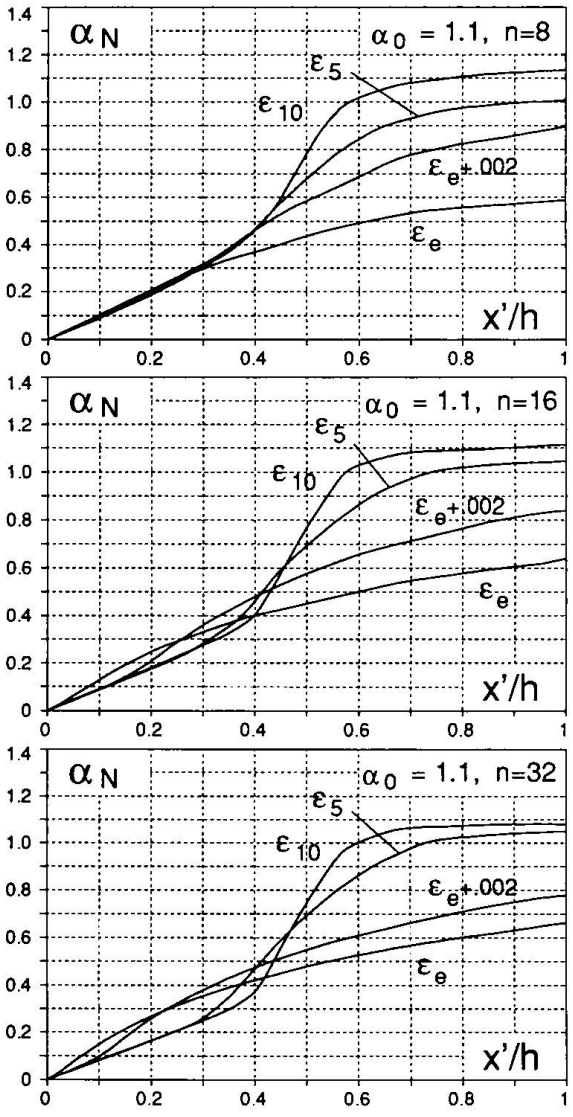

Fig. 4 Values of α_N

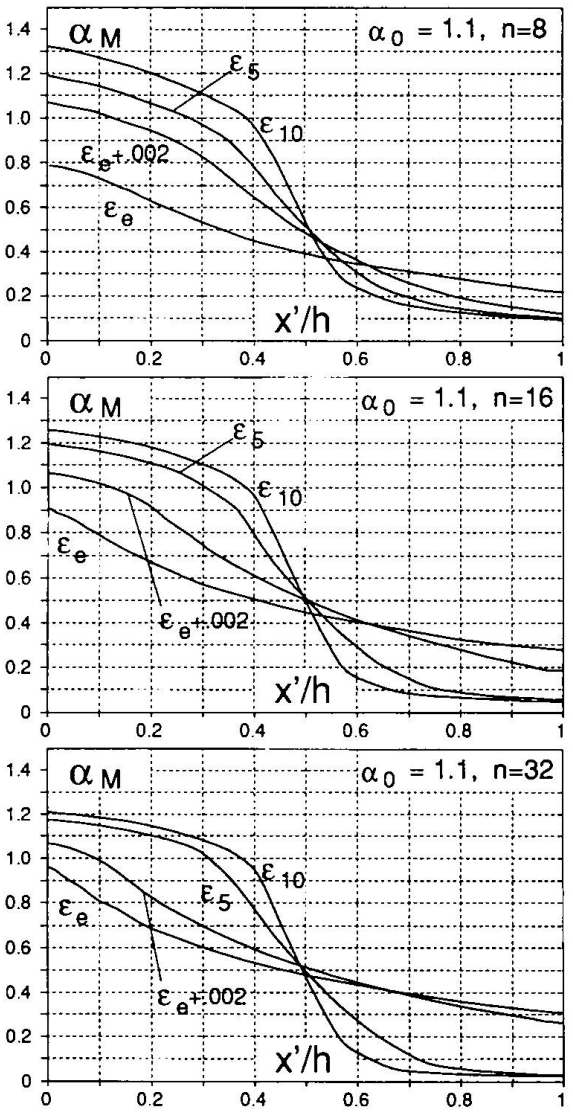

Fig. 5 Values of α_M

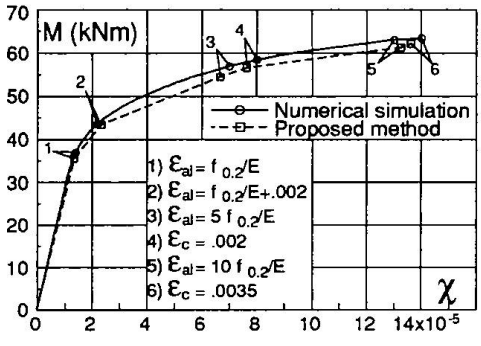

a)

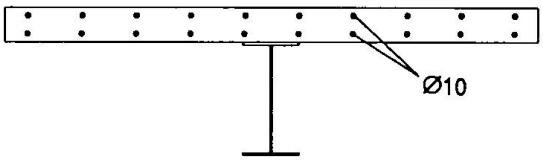

H = 260mm	A = 1494mm²	f'c = 25N/mm²
B = 1000mm	As = 785mm²	fy = 380N/mm²
d = 60mm	A's = 785mm²	f0.1 = 215.6N/mm²
h' = 100mm	ds = 140mm	f0.2 = 223.6N/mm²
h'' = 100mm	d's = 120mm	nR.O. = 19.1

b)

Fig. 6 Comparison of the procedure proposed with numerical simulation.

5. Conclusive remarks

The study presented in this paper represents the logical development of the extensive research work carried out by the Authors on this topic and referred to in [1 to 5]. In those papers, the problem has been faced both from experimental and numerical point of view. Some tests were performed in order to calibrate suitable numerical simulation procedures, which have been successfully used to investigate many aspects of these structures, such as the elastic and post-elastic behaviour, the ductility features, the influence of slab reinforcements, and so on.
The reliability of these simulation methods is the basis of the procedure presented herein. This may be considered as a first approach to the direct estimation of load bearing capacity of aluminium-concrete sections in bending. The difficulty in evaluating the inelastic material response has been overcome through a preliminary numerical study of the aluminium section, which has led to a graphical representation of the section behaviour as a function of the relevant parameters. The existing literature on r.c. structures, including many design manuals, can be profitably used for the prediction of concrete inelastic behaviour. The method proposed is conservative, simple and relatively easy to apply, even though the iterative procedure for the evaluation of the neutral axis position can result in some difficulty when the designer is working without computer aids. Nevertheless, in spite of these achievements, several aspects related to the bending behaviour of this structural typology, namely the effect of the different values of the thermal expansion coefficient, as well as the influence of concrete shrinkage, still remain to be clarified. In addition, the study of the section in simple bending does not exhaust the investigation on the structure regarded as a whole, because the collapse of a composite structure can be also a consequence of other phenomena, such as, for example, the shear brittle failure of the concrete slab, the failure of connectors, the buckling of compressed parts, etc. It is advisable, therefore, that new research can be devoted to this subject in future.

References

[1] Bruzzese, E., Cappelli, M., Mazzolani F.M.: "Experimental Investigation on Aluminium-Concrete Beams", Costruzioni Metalliche, n. 5, 1989.
[2] Bruzzese, E., De Martino A., Mandara A., Mazzolani F.M.: "Esame dei parametri comportamentali del sistema misto alluminio-calcestruzzo", Proc. of the XII C.T.A. Congress, Anacapri, 1989 (in Italian).
[3] Bruzzese, E., De Martino A., Mandara A., Mazzolani F.M.: "Aluminium-Concrete Systems: Behavioural Parameters", Proc. of the International Conference on Steel & Aluminium Structures - ICSAS 91", Singapore, 1991.
[4] Bruzzese, E., Mandara A., Mazzolani F.M.: "Sulla duttilità del sistema misto alluminio-calcestruzzo", Proc. of the XIII C.T.A. Congress, Abano Terme, 1991 (in Italian).
[5] Mazzolani, F.M.: "Aluminium Alloy Structures", FN & SPON, London 1995.

Composite Bridges: Ductility versus Brittleness

Peter TANNER
Research Engineer
IETcc-CSIC
Madrid, Spain

A graduate of ETH Zurich, in 1989, Peter Tanner joined ICOM of EPF Lausanne. Since 1992 he has worked with consultants before joining the Institute of Construction Science IETcc-CSIC. He is a member of the Project Teams for the Spanish steel- and composite bridge code and the code for concrete structures.

Juan Luis BELLOD
Civil Engineer
CESMA, S.L.
Madrid, Spain

Juan Luis Bellod received his civil engineering degree from Technical University of Madrid in 1983. Since 1984 he has worked with consultants in Madrid before founding his own consulting company. He is a member of the Project Teams for the Spanish steel- and composite bridge code and the code for concrete structures.

Summary

Current design methods for composite bridges are stress oriented, which includes the risk of in-built brittle behaviour. Starting with an example which shows that the traditional approaches can lead to unsafe structures, this paper presents a strain oriented design method, suitable for ductility evaluations. Since cross-section ductility is governed by the response of steel compression elements, their analysis requires special attention: a strain oriented approach is introduced for the calculation of load shortening curves of unstiffened and stiffened compression plates.

1. Introduction

Current design codes for composite structures generally use a system of classes to define the ductility of cross-sections, the class of a section being a function of its geometry, stress distribution and the steel grade. The class of the section dictates allowable methods of global analysis (including moment redistributions limited to fixed values) and resistance calculations. In most composite bridges the width to thickness ratios of the steel flange in compression or the part of the steel web in compression is such that the corresponding cross-sections belong to the least ductile class according to the classification system of current design codes (class 4, slender cross-sections, in [1]). Following the approach from these codes, structures with slender cross-sections require elastic global analysis and resistance moments are calculated by using the theory of elasticity and by taking into account the effects of local buckling [1]. If a cross-section shows an elastic behaviour as assumed in the analysis method, then its failure mode is brittle: due to instability phenomenons of the steel sections at internal supports an abrupt decrease of the resistance moment following the attainment of the peak value is observed for increasing rotations (curvatures) (Figure 1a). Cross-sections in the span, on the other hand, are able to undergo large rotations maintaining the maximum value of the resistance moment, they are ductile (Figure 1b).

Brittle structures are very sensitive to the uncertainties of action effects, including those due to creep, shrinkage, temperature, settlement and earthquakes [2], which is illustrated for a bridge with the span arrangement and the cross-sections from Figure 1. From the geotechnical study it can be concluded that no settlement is to be expected for the end supports. The load arrangement according to Figure 1 governs the design of the cross-section A-A following the design philosophy of current codes [3, 4] (Figure 2a). However, one year after the completion of the bridge a settlement of δ=0.1 m of one of the end supports is observed (Figure 1). The governing load arrangement including the effect of the settlement results in an interaction between shear force, V, and bending moment, M, such that the support cross-section A-A no longer reaches the required structural safety level according to the codes [3, 4]: the design action effects are bigger than the design resistance (Figure 2b). Due to the expected behaviour of the support cross-section (Figure 1a), the structure is potentially brittle after the settlement, which means that it can fail

abruptly without previous warning. In order to avoid the design of brittle structures, the traditionally stress oriented design methods are substituted by a strain oriented reasoning [2].

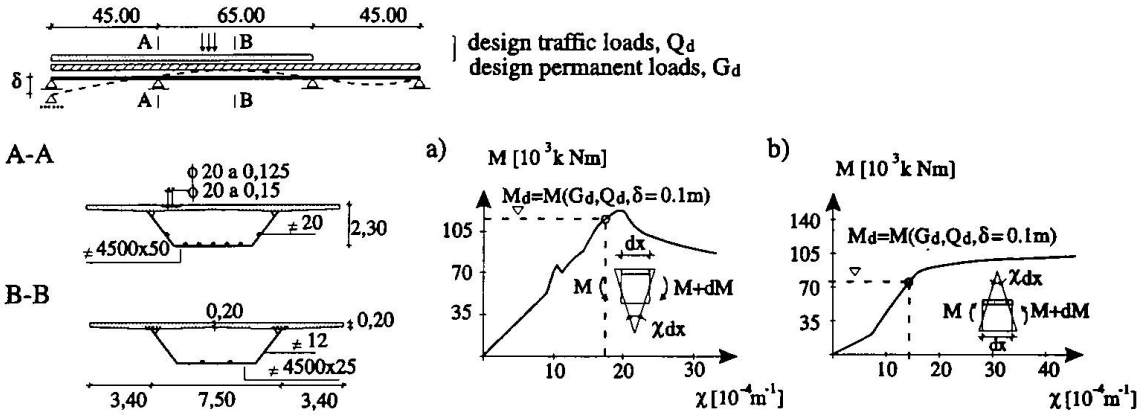

Fig.1 Composite box girder bridge with typical cross-sections and their behaviour in terms of moment vs. curvature, a) at the support (section A-A), b) in the span (section B-B).

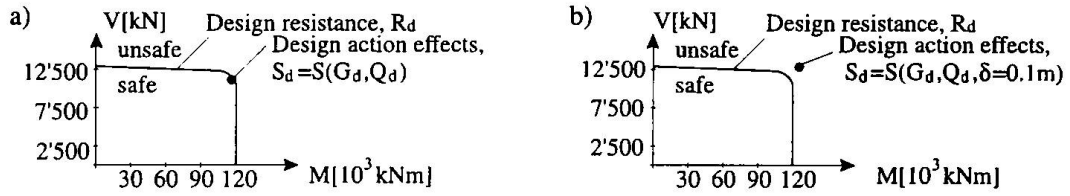

Fig.2 Sensitivity of brittle cross-sections to the uncertainties of action effects: structural safety of the support cross-section A-A from figure 1, a) without, b) with settlement.

2. Strain oriented reasoning

2.1 Overview

2.1.1 Response of cross-sections

Composite box and plate girder bridges subjected to bending moments are composed of different steel plated elements and a concrete slab. A cross-section at an internal support (hogging bending), for example, is composed of the steel compression flange, the reinforced concrete tension flange and the steel webs subjected to bending and axial forces. It is assumed that the behaviour of the different elements composing the cross-section can be modelled independently in terms of load strain curves in the case of the compression- (chapter 3) and tension flanges, and as moment-curvature diagram in the presence of an axial force, in the case of the webs [2]. If the response of the elements composing a cross-section is known, the response of the whole cross-section can easily be obtained: considering different states of strain, the moment-curvature diagram can be established point by point following an iterative calculation procedure [2, 5].

2.1.2 Non-linear analysis

If the behaviour of the bridge cross-sections can be modelled in terms of moment-curvature diagrams (including falling branches in the M-χ diagram of cross-sections in the hogging bending region), the aforementioned redistributions of bending moments (chapter 1) according to these diagrams can directly be taken into account. For this, a non-linear global analysis must be carried out for the calculation of the internal forces and moments. For failure, there is no need to introduce a first yield criteria as usual in bridge design. Allowance can be made for strains in structural steel elements of beyond those corresponding to the yield strength of the steel, ε_y. This implies necessarily additional serviceability checks [4, 5].

A non-linear analysis carried out for the example from chapter 1 shows that in spite of the settlement of δ=0.1 m of one end support no structural failure is to be expected (Figure 1). For the failure criteria from [4, 5], settlements of up to δ=0.3 m could be justified by a non-linear analysis [6]. However, even though non-linear analysis is possible with modern numerical tools it is only considered viable in special cases. Therefore, an alternative design method which is aimed at the practising engineer for everyday use is proposed in 2.1.3.

2.1.3 Ductile structures

If instability phenomenons of the steel member govern the behaviour of a composite cross-section, its failure mode is brittle (Figure 1a refers to a box girder; in the case of plate girders the falling branch of the M-χ diagram may be steeper due to possible lateral torsional buckling). If, on the other hand, the tension flange yields before the compression flange reaches its ultimate strength, the corresponding cross-section shows a ductile behaviour which is typically the case for composite cross-sections in sagging bending regions (Figure 1b). However, if in the hogging bending region the neutral axis is near to the compression flange, important gains in section ductility are possible [2, 5, 7]. Consequently, the criteria for a ductile behaviour of a cross-section is that the tension flange reaches its maximum strain before the compression flange fails.

If a ductile behaviour of both, the cross-sections in the span and at the support can be guaranteed, then there is no need to carry out a non-linear global analysis (2.1.2): applied moments can be determined by using elastic global analysis which is the common practice in bridge design. Resistance moments may be deduced from the moment-curvature diagrams, which are needed to ensure that the ductility criteria is satisfied and which are calculated according to the strain oriented approach from 2.1.1. In a ductile bridge structure moment redistributions are possible. Therefore, their sensitivity to the uncertainties of the action effects is considerably reduced. If in the example from chapter 1 the cross-section at the support would show a ductile behaviour, settlements of even more than δ=0.3 m (2.1.2) would not reduce the structural safety below the required level according to [3, 4].

2.2 Validity of the method

The proposed strain oriented method, based on the separate modelling of the different elements composing a cross-section only is valid if possible negative reciprocal influences between the elements due to instability effects can be excluded. Furthermore, it is to be ensured that the different elements behave as is implicitly supposed in the design models. The assumed structural behaviour can be guaranteed if a set of geometrical minimum requirements are reached [2, 4, 5].

3. Unstiffened and stiffened steel plates under compression

3.1 Introduction

The behaviour of composite bridge cross-sections depends very strongly on the response of their steel plated elements under compression. Due to different possible instability effects, the analysis of these elements is complex and requires special attention. Most design codes only give rules for the calculation of their ultimate load. The presented strain oriented approach requires, however, an easy-to-use method which allows for an accurate estimation of the load shortening behaviour of steel plated elements. The cases of unstiffened and stiffened plates are considered separately.

3.2 Unstiffened steel plates

3.2.1 Strain oriented formulation of the effective width approach

Due to a membrane effect unstiffened steel plates under compression possess a post-critical resistance which can be taken into account according to the effective width concept [8]. Appropriate buckling curves (e.g. Winter [8]) are introduced for the modelling of geometrical imperfections and residual stresses. The effective width, and consequently the resistance, of such elements is strain dependent: the bowing effect (out-of-plane deflection) increases with increasing strains, which means that the effective width and the resistance decrease after having reached a

maximum value. The strain dependence of the resistance can be taken into account by reformulating the effective width approach for steel compression plates [5]:

$$b_e = \rho \cdot b = \left(\frac{\overline{\lambda_p} - 0.22}{\overline{\lambda_p}^2} \right) b \qquad (1)$$

b_e effective width
b total width of the plate
ρ reduction factor for plate buckling

In the well known expression for the reference slenderness, $\overline{\lambda_p}$, stresses are substituted by strains:

$$\overline{\lambda_p} = \sqrt{\frac{\varepsilon}{\varepsilon_{cr}}} \qquad (2)$$

ε applied strain
ε_{cr} critical buckling strain of the plate according to linear buckling theory [8]

3.2.2 Results

In the present section, the load shortening curves of unstiffened steel plates which are established by using the proposed strain oriented effective width approach are compared to available results [8] from tests and detailed numerical simulations. Major parameters affecting the behaviour of such elements are discussed. These parameters are: residual stresses, aspect ratio and initial out-of-plane deflections. The obtained results show that the proposed method is applicable for design purposes [5].

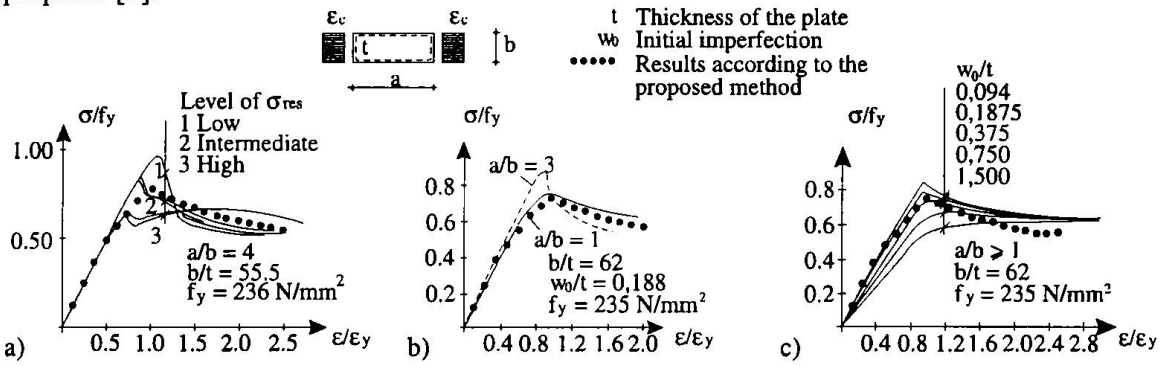

Fig.3 Strain oriented effective width approach - comparison with test results: influence of a) residual stresses, σ_{res}, b) aspect ratio, a/b, c) initial imperfections, w_0.

Moxham [8] tested simply supported compression plates with an aspect ratio of a/b=4, different levels of residual stresses, σ_{res}, and without nominal initial deflections, w_0=0. Even though the proposed method takes simultaneously into account the influence of residual stresses and initial deflections, a direct comparison with the test results is possible: for a plate slenderness of b/t=55.5, as used in the tests, the influence of the residual stresses tends to mask the one of the geometrical imperfections [8]. The proposed method leads to results which almost coincide with the obtained test results for an intermediate residual stress level (Figure 3a).

Frieze [8] showed that minimum plate strength is obtained for plates with an aspect ratio of approximately a/b=1. Longer plates exhibit higher maximum values of the strength, higher prepeak stiffness and less ductility (Figure 3b). The results calculated by using the proposed method are very close to the ones obtained by Frieze for square plates.

Figure 3c) shows the influence of the variation of the initial deflections, w_0, on the behaviour of a plate without residual stresses, σ_{res}=0 [8]. Again, a direct comparison is possible although in the proposed method residual stresses and initial deflections are simultaneously taken into account: for a plate slenderness of b/t=62, the influence of initial deflections dominates over the residual

stresses [8]. The results according to the proposed method correspond to an intermediate level of initial deflections, which is in the range of the fabrication tolerances in current codes [4].

3.3 Stiffened steel plates

3.3.1 Strain oriented strut approach

In orthogonally stiffened compression plates different buckling modes are possible: overall buckling, nodal buckling of the plate panels between longitudinal stiffeners, tripping of stiffeners with open cross-sections and all possible combination modes. Practical geometries of compression flanges in composite box girder bridges usually lead to column type failure [8]. This failure mode can be guaranteed by respecting so called minimum requirements (2.2). The load shortening behaviour can therefore be obtained by using a model based on the strut approach (Figure 4). The proposed model treats the stiffened plate as a serie of disconnected struts consisting of a stiffener and an associated plate width [4, 5]. The ultimate load of a stiffened plate, N_{ult}, is the sum of the ultimate load of these struts and the ultimate load carried by the panels at the supports of the longitudinal edges (Figure 4):

$$N_{ult} = \left[n \cdot \chi\left(\rho \cdot b_L \cdot t + A_L\right) + \rho \cdot b_L \cdot t\right] f_y \qquad (3)$$

n	number of longitudinal stiffeners
b_L	width of the panel between two longitudinal stiffeners
t	thickness of the plate
A_L	area of the cross-section of a longitudinal stiffener
f_y	yield strength
ρ	reduction factor for plate buckling of the subpanels
χ	reduction factor for buckling of the struts

The interaction between the buckling of the struts and nodal buckling is taken into account by an iterative calculation of ρ (according to (1)) and χ (according to european column buckling curve c [4]). For this purpose, the applied strain, ε, in the reference slenderness of the subpanels for the calculation of ρ according to (2) is substituted by $(\chi \cdot \varepsilon_y)$, where ε_y is the yield strain of the material [4, 5].

In order to obtaining the load shortening curve, it is assumed that the ultimate load, N_{ult}, is reached for an intermediate strain, ε_{ult}, between the ultimate strains of an unstiffened plate and the one of a steel column, respectively [5]. For the prepeak behaviour, a linear load shortening relation is assumed until first buckling occurs, usually nodal buckling between longitudinal stiffeners (Figure 4). The postpeak behaviour is described by using well known relations between load and deflections of ideal rigid plastic columns.

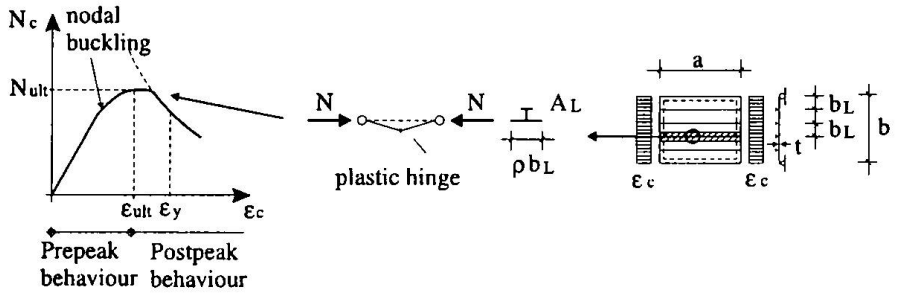

Fig.4 Stiffened compression plates - strain oriented approach.

3.3.2 Results

Ghavami tested longitudinally stiffened steel compression plates with and without transversal stiffeners up to collapse [9]. In [5], the results of 12 of these tests are compared to the results obtained by using the proposed model for the ultimate load, N_{ult}. For comparison, the ratio between the ultimate load according to the model and the collapse load from the corresponding test is established for each of the 12 results. For the analysed sample, a mean value for this ratio

of m=0.97 is found, and a standard deviation of s=0.055. These results are very satisfactory: the model produces slightly conservative results (m<1), and the found scatter is very small (coefficient of variation cov=0.056) compared to usual scatters produced by other design approaches for stiffened compression plates [9].

4. Conclusions

The rules given in current design codes for composite bridge structures are simple to use but do not include all relevant parameters for the representation of section ductility. Therefore, the beam load capacity can not be accurately predicted, and in-built brittle behaviour can not be excluded in the design. In order to avoid these drawbacks, ductility or rotation-capacity evaluations for cross-sections are necessary, which is possible if the traditionally stress oriented design philosophy is substituted by a strain oriented reasoning. Benefits of a ductile structural behaviour include that the sensitivity of a structure to the uncertainties of action effects is reduced.

The proposed strain oriented design method is suitable for a uniform treatment of all cross-sections and allows for the evaluation of moment-curvature diagrams in a way which is applicable for design purposes. Ductile structural behaviour can therefore be guaranteed.

Acknowledgements

Some of the presented work has been carried out as a part of the studies for the Spanish Recommendations for the design of steel and composite bridges, promoted by the "Dirección General de Carreteras" of the Ministry of Public Works.

References

1. ENV 1994-2 (Second Draft). Design of composite steel and concrete structures. Part 2: Bridges. European Committee for Standardisation, Brussels, July 1996.
2. RUI, X., TANNER, P., BELLOD, J.L., CRESPO, P. Towards a consistent design method: A proposal for a new steel and composite bridge design code for Spain. Stockholm, Swedish Institute of Steel Construction, Publication 150 Vol. I, 1995. ISBN 91-712-009-4
3. IAP-96 (Draft). Actions on road bridges. Ministry of public works, Madrid, 1996. (in Spanish)
4. RPX-95. Recommendations for the design of composite bridges. Ministry of public works, Madrid, 1996. (in Spanish)
5. TANNER, P. Design of steel plated structures according to the Spanish recommendations RPM/RPX-95. Working Paper, 27th meeting of European Convention for Constructional Steelwork - Task Working Group 8/3, ECCS-TWG 8/3, Barcelona, March 4-5, 1996.
6. BELLOD, J.L. and GOMEZ NAVARRO, M. Some thoughts on non-linear analysis of composite bridges. Proceedings Composite Bridges - State of the art in technology and analysis. 2nd International meeting. (Martínez Calzón, Ed.), Madrid, 1996. (in Spanish)
7. KEMP, A.R., TRINCHERO, P. and DEKKER, N. Ductility effects of end details in composite beams. In: Composite construction in steel and concrete II. (W. Samuel Easterling, W.M. Kim Roddis, Eds.), Potosi, Missouri, 1992. ASCE, New York, 1993.
8. ECCS. Behaviour and design of steel plated structures (P. Dubas and E. Gehri, Eds.). European Convention for Constructional Steelwork (ECCS n° 44), Brussels, 1986.
9. GHAVAMI, K. Experimental study of stiffened plates in compression up to collapse. Journal of Constructional Steel Research, 1993.

The Design Approach for a New Composite Space Frame Bridge System

John M.C. CADEI
Principal Engineer
Maunsell Structural Plastics
Beckenham, UK

John Cadei graduated in Civil Engineering from Imperial College, London. He is an expert in the design and analysis of large structures and advanced materials.

Allan E. CHURCHMAN
Managing Director
Maunsell Structural Plastics
Beckenham, UK

Allan Churchman received a Civil Engineering Degree from the Univ. of Surrey. He has been responsible for major bridge projects and structures in advanced composite materials.

Summary
This paper describes the design approach to SPACES, a new bridge system comprising a tubular steel space frame, participating roadway slab, and an enclosure shell in advanced composite material. The system, which is suitable for girder bridges over 40m in span and long span cable-supported bridges, affords steel weight savings of up to 50%, and significant benefits in life-cycle costs . Bridge configuration criteria, structural behaviour, simplified methods of analysis , and design criteria for key elements are presented.

1. The bridge system

The SPACES bridge system combines an optimised steel space frame, a concrete roadway slab acting compositely with the space frame, and a corrosion-free enclosure shell in advanced composite material which permanently protects the steelwork against corrosion (Fig. 1). The system is designed to provide competitive solutions on a life-cycle cost/benefit basis to a broad spectrum of bridging needs for highways, railways, and footways, ranging from girder bridges and viaducts over 50 m in span to long span cable-supported and overhead arch bridges. The system and its advantages for the owner and end-user have been described in Ref. 1, 2.

The space frame is normally configured as a double-layer rectangular grid connected by diagonal braces arranged on a tetrahedral pattern (Fig 2). It is an all-welded structure fabricated from tubular steel members connected either directly to each other or to cast steel nodes. The space frame acting compositely with the roadway slab is an efficient structural form which affords material and fabrication savings over conventional forms of steel bridge construction such as plate girders, stiffened box girders, and trusses formed from fabricated sections, for spans greater than 50 m.

The enclosure shell is formed from interlocking modular FRP components having the strength and stiffness to constitute a permanent structural platform for inspection and maintenance (Ref. 3). It is attached to the underside of the steel space frame by a system of hangers. It may be shaped to achieve particular architectural or aerodynamic objectives, and may be conformed to a variety of bridge alignments. Depending on the specific requirements of the application it can be made to participate structurally with the rest of the structure to increase its torsional rigidity.

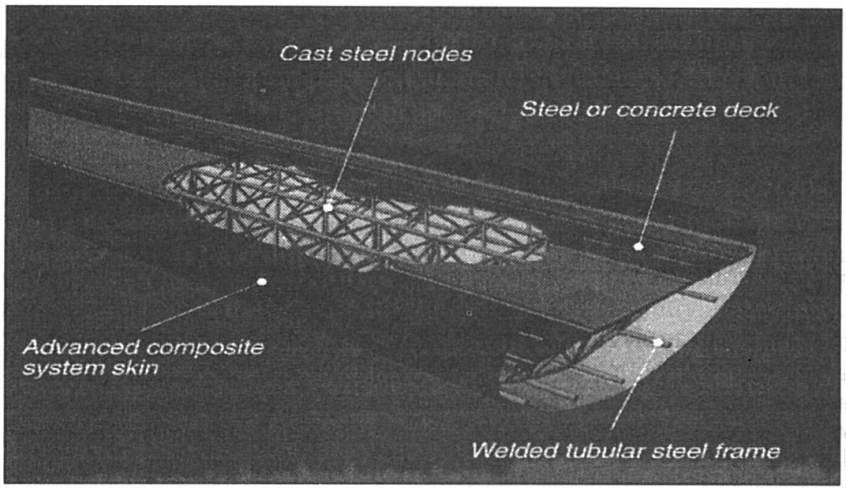

Figure 1 SPACES System Technology

2. Bridge configuration

The objective sought in the geometric configuration of the space frame is to achieve maximum regularity and repetition of standard modules along with well-conditioned node geometry, within the overall functional and aesthetic criteria informing the design of the bridge. The space frame grid and the enclosure can be readily configured for bridges skewed or curved in plan. The direction vector of the space frame diagonals (Lx, Ly, Lz) is selected to minimise the node and member density, thereby improving fabrication economy; and render the angles between members suitable from the point of view of node geometry and ease of fabrication. The relationship of tube diameters is selected to avoid intersection of brace footprints at nodes, maximise node strength, and facilitate automated cutting and welding. The deck span/depth ratio is chosen to optimise the weight of steel.

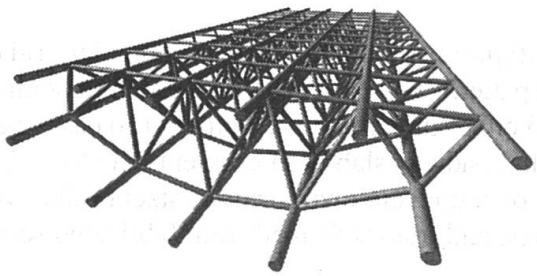

Figure 2 Space frame configuration

In girder bridges, the longitudinal chords are normally the primary members and may therefore run continuously through nodes with the other members branching off . In cable-supported bridges where there is more significant biaxial bending, chord sizes are sometimes varied across a section in order to achieve a clear separation between diameters of intersecting longitudinal and transverse chords, so as to maximise joint strength and fatigue resistance.

Cast steel nodes are used where dictated by joint strength or fatigue endurance requirements, typically at points of high transverse load such as at bearings and in hogging moment regions of continuous viaducts. Diagonals are welded directly onto primary chord members or onto node

stubs. The cost of cast nodes is a function of the external volume of the nodes. Therefore one aims to minimise the diameter of the principal chords by adopting the minimum permissible diameter/thickness ratio in the most heavily loaded member.

3. Structural performance

A naked rectangular grid space frame as used for roofs possesses considerable longitudinal and transverse stiffness due to the bi-directional array of chords but has negligible torsional stiffness. Moreover, if not properly restrained externally, it can have a low global buckling strength due to lack of in-plane stiffness of the compression grid. However when the top grid is combined with a participating concrete slab, the structure acquires considerable torsional stiffness and global buckling strength. The high torsional stiffness results in negligible torsional rotation of the deck under eccentric lane loading, leading to a uniform distribution of stress between longitudinal chords, the torsional moment being absorbed primarily by forces in the brace members. The combination of high transverse and torsional stiffness gives the deck an excellent ability to distribute concentrated loads from vehicle axles and abnormal vehicles, thereby reducing fatigue stresses and other local effects. It also renders the deck particularly suitable for cable-supported bridges, where biaxial bending is more significant than in girder bridges and torsional stiffness may be required for adequate aeroelastic stability. The triangulation in the transverse plane ensures that the cross-section is relatively free from distortion.

As a result of the slab acting as a stiff shear plate in its own plane and the tetrahedral arrangement of braces, all the nodes are effectively restrained laterally. Hence the global critical buckling mode is limited to local buckling of members between nodes. Given the relatively low slenderness ratio of the tubular members, they can mobilise a high proportion of their yield strength in compression. This is in contrast to traditional thin-walled steel bridge structural forms based on steel plate and stiffeners, in which as the depth of the structure increases, the plates become progressively weaker in buckling, and the stiffeners, which do not make very efficient use of material, become increasingly heavier, with a significant penalty in material usage. As a result, it has been found that in the 100 m span range, the weight of steel in SPACES decks approaches 50% of that in a conventional steel box girder structure.

Tubular members have the advantage of optimum compressive capacity in relation to weight, of being available in a much wider range of weights than rolled steel sections, and of enabling three-dimensional joints to be readily formed without the need for complex fabrications involving stiffeners and corrosion traps. The lower slenderness of tubular brace members compared to equivalent stiffened plates also results in higher local natural vibration frequencies. As result there is less noise emission in dynamically loaded structures such as high speed railway viaducts.

4. Modelling and analysis

Due to the resistance of the cross-section to distortion, the structure may be analysed accurately enough for preliminary design purposes as an equivalent beam for global effects and an equivalent orthotropic plate for local effects of concentrated loads. The stiffness properties of the beam and plate can be readily determined by imposing the displacement field for the deformation mode associated with the stiffness property of interest, applying the virtual work or minimum strain energy method to determine any unknown modal parameters (e.g. in the case of the torsional mode, co-ordinates of shear centre and nodal values of warping functions), and using equilibrium to obtain the stiffness value. The properties of interest for the beam model are the flexural and shear stiffnesses EI, and GA_s and the torsional and warping stiffesses GK and EI_w, while for the orthotropic plate model the parameters are flexural stiffness D_{xx}, D_{yy}, D_{xy}, D_{33}, and shear stiffnesses S_x, S_y.

Critical loading patterns and magnitudes are determined from beam influence lines and plate and orthotropic plate influence surfaces which are readily obtained. Once the stress resultants in the equivalent continuous structure have been calculated by the usual methods of structural analysis (with a significantly reduced number of degrees of freedom), the stress resultants in the space frame members and the concrete slab may be derived on the basis of the modal distribution of member forces determined during the calculation of the modal stiffness parameters . Thus an apparently complex structure, having a large number of degrees of freedom, can be analysed by simple methods which can be carried out manually or implemented on a spreadsheet, yielding results typically within 5% of a more accurate analysis.

For detailed design, the structure is analysed by the finite element method. The space frame members are modelled as three-dimensional beams and the slab by shell elements at the appropriate eccentricity from the top grid members. When used compositely the enclosure is modelled by anisotropic shell elements. Joint elements may be used to represent the shear connectors if required. By virtue of the regularity and repetitiveness of the structural configuration, finite element models can be generated automatically with simple macros. The advantage of finite element modelling is that colour-coded stress resultant contour plots may be produced for specific families of elements (e.g. chords or braces), which can be also read as tube size distribution maps (Fig. 3). The ease with which tube sizes can be varied to suit the load envelope pattern is another reason for the structural efficiency of the composite space frame. The finite element modelling takes into account the stage-by-stage incremental build-up of the structure, with the concrete slab being typically applied in various stages after the erection of the space frame.

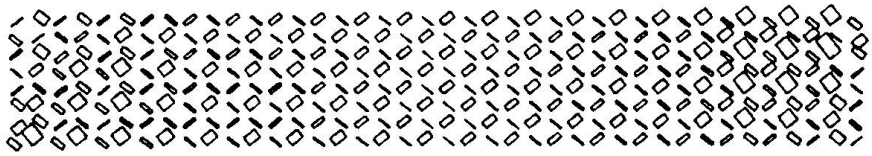

Figure 3 Typical brace maximum axial load 'contour' plot

Structural elements are designed for strength considering factored extreme load effects and ultimate strength, and for fatigue and durability under actual load spectra. Nodes are designed for strength and fatigue using when applicable parametric strength equations given in such references as [Ref 4 - 7], modified for multiplanar joints [Ref 5]. Otherwise nodes are analysed by finite element analysis, assuming the Von Mises yield criterion in the strength analysis and the hot spot stress criterion as defined in BS 7608:1993 in the fatigue analysis.

5. Contribution of enclosure shell

The primary purpose of the enclosure is to provide long-term corrosion protection to the tubular space frame and access for inspection and maintenance. In terms of material, it is typically equivalent to a 10 mm thick plate weighing 20 kg/m^2 and the elastic properties of the e-glass/polyester composite material are in the order of E_x= 20 GPa, E_y= 8 GPa, ν_{xy}= 0.18, G_{xy}= 4.0 GPa. The shell is not normally required to act compositely with the space frame, but can be made to do so if advantageous for the application. When not acting compositely, the fixings and joints are designed to accommodate relative movements between the steel and the composite. If connected so as to act compositely, the enclosure has little impact on the longitudinal stiffness of the lower grid because of its low longitudinal modulus and area. However in applications in which the lower grid is not triangulated, and therefore does not possess significant shear stiffness, the enclosure shell can make a significant contribution to the global torsional stiffness of the deck, increasing it by up to 50%.

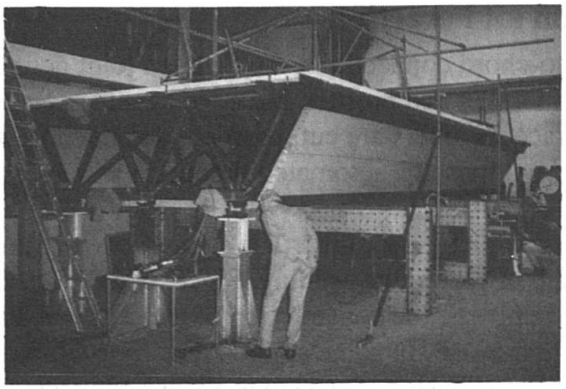

Figure 4 Cambridge half scale model of SPACES deck

Tests were carried out at the University of Cambridge [Ref ...] on a half scale model of a composite space frame deck (Fig. 4), which demonstrated that in that instance the shell increased the torsional stiffness by about 50% (Fig. 5). Clearly in larger bridges the enhancement would be less, and in general when it is necessary to increase the shear stiffness of the lower grid it is sometimes more economic to do so by adding in-plane bracing. The difference between the experimental and predicted response with the participating shell is due to the slack in the connections.

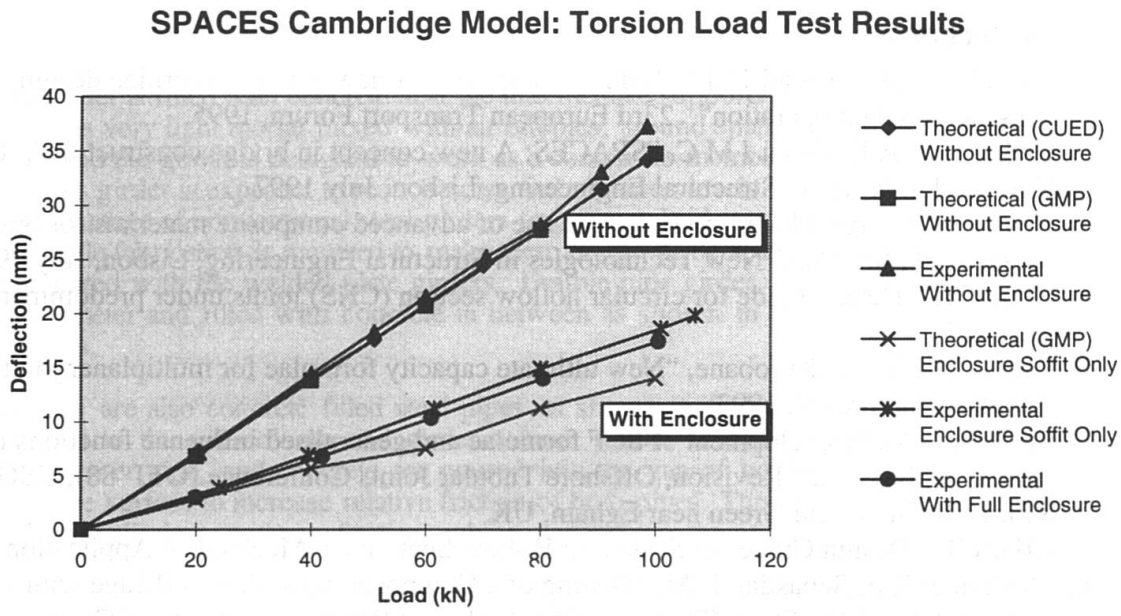

Figure 5 Comparison of experimental and theoretical results with and without participation of FRP shell

6. Design for fabrication and erection

In the case of welded brace-to-chord connections, the detailed joint geometric data needed to define continuously variable member end profiles and edge bevel angles is calculated by computer programme. The brace members are cut, profiled, and bevelled by automatic milling machines. Welding is carried out by semi-automated processes where convenient.

The space frame is erected in complete span units. The rigidity of the frame makes it possible to achieve good fit-up to facilitate in-place butt welding. Since SPACES decks are usually continuous over intermediate supports, the construction of the concrete slab is sequenced to minimise permanent tension in the slab. In some applications post-tensioning cables are used within the space frame to prestress the slab. The slab is always connected to the longitudinal chords by shear connectors and may also be connected to the transverse chords in the case of larger grid sizes to increase 2-way spanning action. Slab panels are typically cast on permanent formwork, which can be propped off the space frame lower grid. When there is a sufficient gap between the slab and the transverse chords, the slab can be cast on a travelling form.

7. Conclusions

A steel space frame acting compositely with a roadway slab is a more efficient structural form than a plate or box girder structure for longer spans. The provision of an enclosure ensures that the space frame members which on account of their spatial orientation could be difficult to maintain are protected from corrosion. The space frame's regular modularity enables rapid design and fabrication. The design approach has been validated by a half-scale model test .

8. References

1. Churchman A E, Cadei J M C, "SPACES System: A new concept in bridge design, construction, and operation", 23rd European Transport Forum, 1995.
2. Churchman A E, Cadei J M C, "SPACES: A new concept in bridge construction", Int. Conf. New Technologies in Structural Engineering, Lisbon, July 1997
3. Head P R, Thorpe J E, Irvine R A "The use of advanced composite materials for bridge enclosures", Int. Conf. New Technologies in Structural Engineering, Lisbon, July 1997
4. CIDECT, " Design guide for circular hollow section (CHS) joints under predominantly static loading"
5. Paul J, Makino Y, Kurobane, "New ultimate capacity formulae for multiplanar joints", Tubular structures V, 1993.
6. Efthymiou M, "Development of SCF formulae and generalised influence functions for use in fatigue analysis", 2nd Revision, Offshore Tubular Joints Conference (OTJ '88), USG Offshore Research, Englefield Green near Egham, UK
7. CIDECT, "Design Guide for Structural Hollow Sections in Mechanical Applications", 1995
8. McConnel R E, Sebastian R M, "Testing of a Composite Space Truss Bridge with GRP Panels", CUED/D - Struct/TR.149(1995), Technical Report, University of Cambridge, 1995

Design and Experiments on a New Railway Bridge System using Concrete Filled Steel Pipes

Tetsuya HOSAKA
Japan Railway Constr. Public Corp.
Tokyo, Japan

Toshio UMEHARA
Japan Railway Constr. Public Corp.
Tokyo, Japan

Shunichi NAKAMURA
Nippon Steel Corporation, Futtsu
Chiba, Japan

Kenji NISHIUMI
Nippon Steel Corporation, Futtsu
Chiba, Japan

Summary

A new railway bridge system has been developed using steel pipes as the main girders, which are filled with concrete or air mortar depending on the span positions, and are also composite with concrete slab. This new girder could be not only economical but reduce noise and vibration induced by trains. Columns and piles are also concrete filled steel pipes. Pipe to pipe joint using concrete is applied to the pile-column and girder-column joints. This new bridge system is widely studied by analysis and experiments, among which three experiments are explained in this paper. Design detail of this bridge system is also presented.

1. Introduction

A new railway bridge system has been developed using steel pipes as the main girders as shown in fig. 1. The pipe girder is filled with concrete near the intermediate supports, whereas it is filled with air mortar, which is very light mortar mixed with air bubbles, around span-center to reduce the self weight. RC slab and the girder is designed to work as a composite member in the positive bending moment zone. This girder is expected to reduce noise and vibration levels induced by trains, which is the main disadvantage of conventional steel girders for railway bridges. Steel pipes are produced at steel mill and little fabrication is required to make them bridge girders, therefore it could be very economical compared with the welded plate girders. Double pipe girder, consisting of two pipes with different diameter and filled with concrete in between as shown in fig.2, could be used for larger span bridges.

Columns and piles are also concrete filled steel pipes as shown in fig. 1. Pipe to pipe joint with concrete is applied to the pile-column and girder-column joints. In this joint the upper pipe is inserted into the lower pipe, and concrete are poured into the gap of both pipes. Spiral ribs are attached on the pipe surface to increase relative friction of both pipes. This joint is very simple and firm, and so it could eliminate concrete footing, which also reduces the construction cost.

This new bridge system is widely studied by analysis and experiments, among which three experiments are reported in this paper: bending tests, shear connector tests and noise tests. This bridge system is to be applied to the planned railway bridges and the design detail is also presented.

2. Bending Tests

Bending tests of pipe girders are carried out by the method shown in fig.3. Two groups of specimens shown in fig.2 are tested. Bending strength and behavior of concrete filled steel pipe

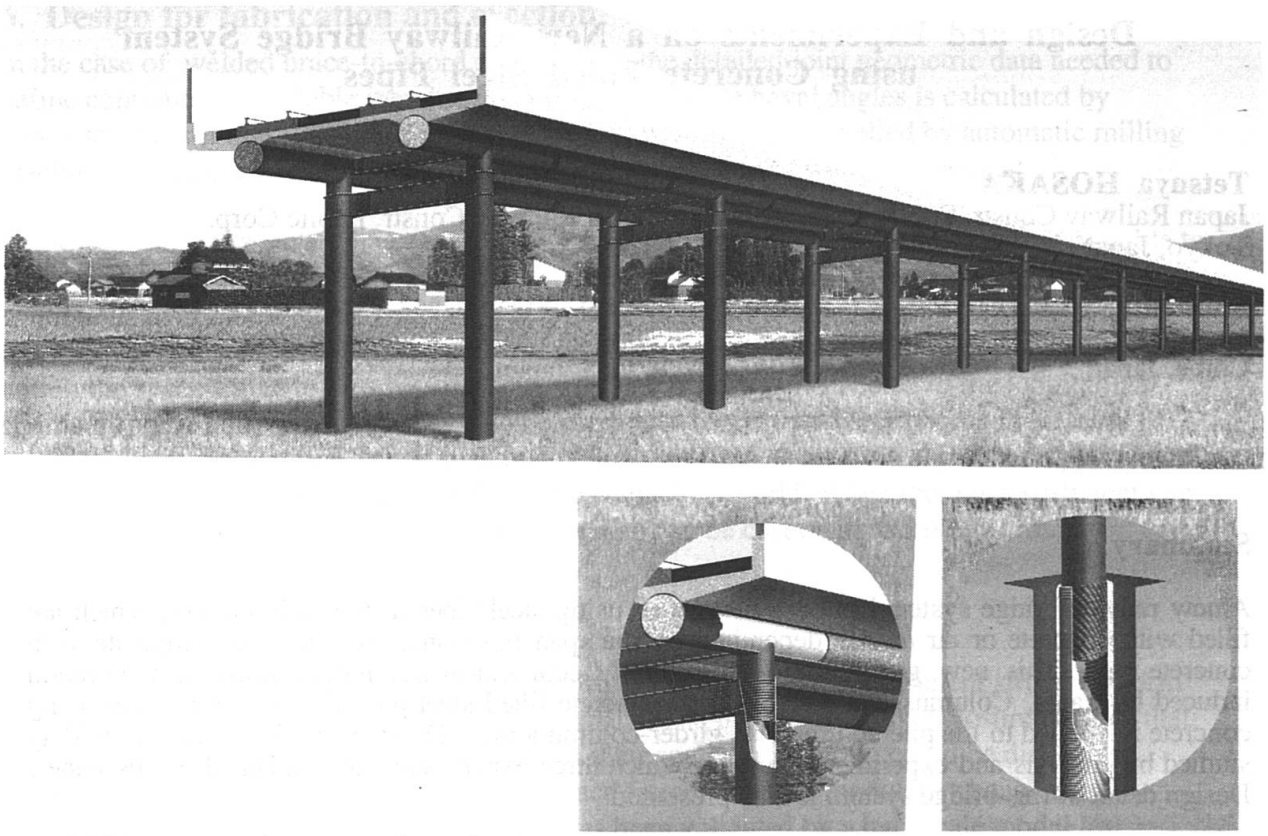

Fig.1 Illustration of a new railway bridge

girders with concrete slab are mainly studied in the first group (T1 to T3). T1 is concrete filled double steel pipe girder, T2 concrete filled double steel pipe girder with concrete slab and T3 steel pipe girder with concrete slab. Bending strength and behavior of air mortar filled steel pipe girders are studied in the second group (M1 to M6). M1 is made only of steel pipe. Air mortar with compressive stress of 7, 14, 57kg/cm^2 , light aggregate concrete with compressive stress of 325kg/cm2 and normal concrete with compressive stress of 460kg/cm^2 are filled in the pipes of M2, M3, M4, M5 and M6 respectively. Density of air mortar of M2, M3 and M4 is 0.50,0.54 and 1.12 respectively.

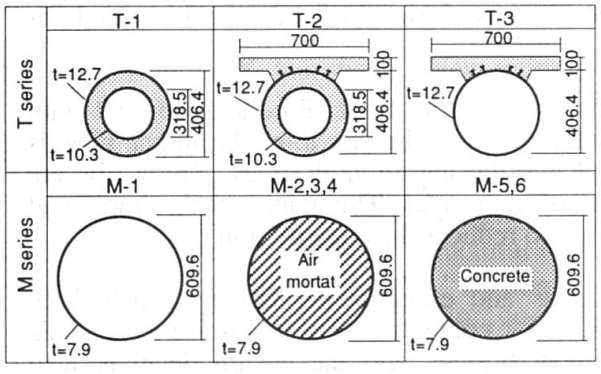

Fig.2Test specimen

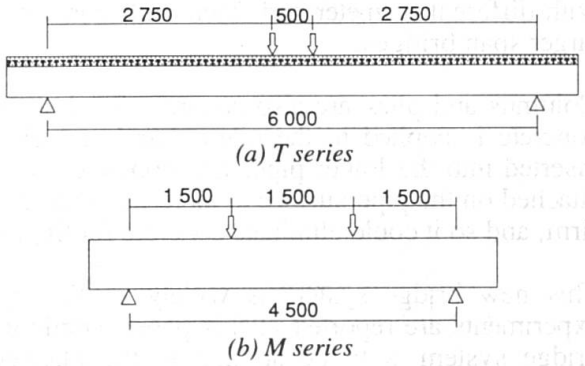

Fig.3Experimental methods

Relations of bending moment and deflection obtained by the first group experiments are shown in fig.4. Bending moment of concrete filled steel pipe girder of T1 and T2 does not seem to decrease even after the maximum point, which demonstrates good ductile property. However, bending moment of T3 decreases relatively sharply after the maximum point. It is thought from these difference that the filled concrete has an important role to restrict the local buckling of the pipe and increase the bending capacity. T2 has the higher initial rigidity among three specimens because of

the RC slab, but just after the yield point the RC slab is collapsed, and therefore the ultimate strength is the same as T1.

Relations of bending moment and deflection obtained by the second group of experiments are shown in fig.5. The maximum bending moment of steel pipe specimen M1 is improved nearly double by the filled concrete in M6 and M5. Air mortar filled specimens M2 to M4 also increase the maximum bending moments, but they are not as large as M6 or M5. However, it should be noted that ductile property is greatly improved in M4 compared with M2 and M3. This means that air mortar with strength over 50kg/cm^2 could restrict the development of local buckling of steel pipe and, therefore, could avoid sharp decrease of bending moment after the maximum point.

Relations of applied moments and strains of slab concrete and filled concrete of T2 are shown in fig.6. Strains of upper and lower slab concrete increase linearly with applied moments in the first stage, but the RC slab collapses when the strain reaches about 3400μ. After this, strain of filled concrete starts to increase sharply, which suggests the neutral axis lowers and filled concrete starts to contribute to the bending capacity. The strain finally reaches at about 4800μ due to so called the confined effects of filled concrete.

Strain distributions of steel and concrete of T2 are shown in fig.7. Strains of inner pipe, outer pipe, slab concrete and slab reinforcing steel bars are on the same linear lines on the different bending moment levels, which suggests these elements behave as one piece. Though, filled concrete behaves differently in the large bending moment levels, and so, adhesion does not seem to exist between pipes and filled concrete. Since the strains of pipes and slab concrete distribute on the linear line, the RC calculation method based on the Bernoulli Euler Principle could be applied. Fig.8 shows experimental data and calculated values by RC method in cases T-2 and T-3. Both values have good agreement within the elastic zone, but the experimental values are about 15% large the calculated values which do not include the confined concrete effect.

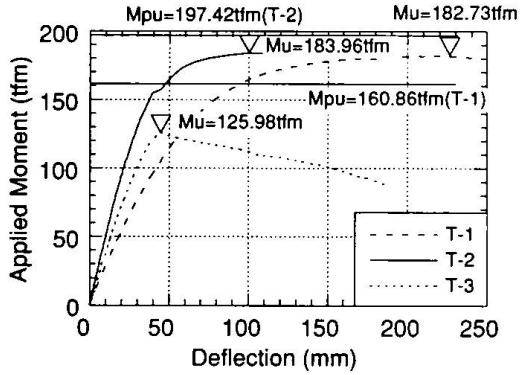

Fig.4 Moment displacement curve (T1 to T3)

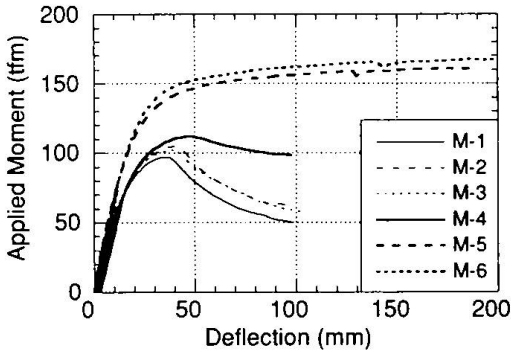

Fig.5 Moment displacement curve (M1 to M6)

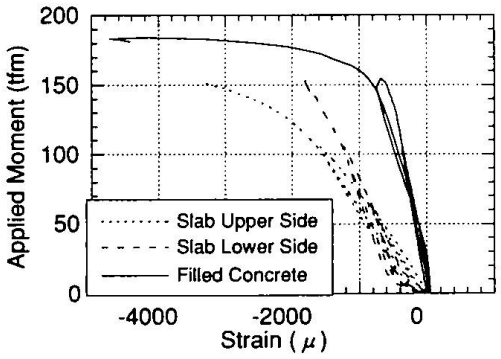

Fig.6 Concrete strain curves (T2)

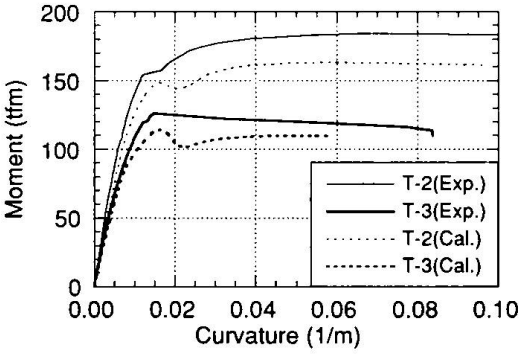

Fig.8 Comparison of experiments and RC calculation(T1 to T3)

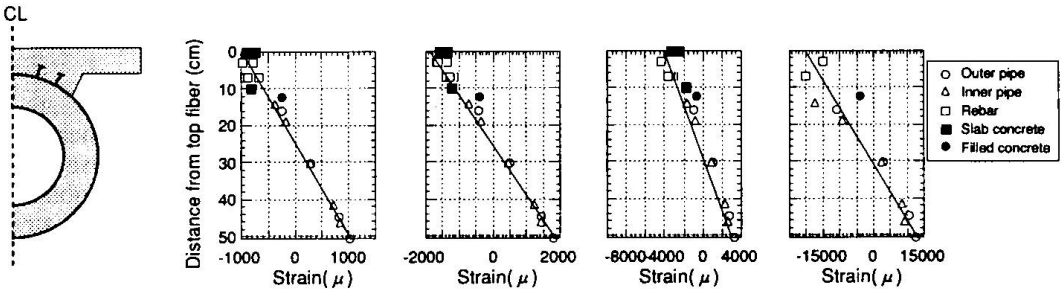

(a) Ma=66.4tfm (b)Md=105.6tfm (c) My=154.4tfm (d) Mu=184.0tfm

Fig.7 Strain distribution (T2)

3. Shear Connector Tests

Concrete slab is connected to the pipe girders with studs, and composite action is expected in the positive bending moment regions. However, the shape of the girder is different from the usual I-girders, therefore the shear strength is studied by the push-out tests as shown in fig.9. Two specimen, double pipe girder (PS-1) and single pipe girder (PS-2), are tested. Fig.10 shows relation of applied loads and relative slip between the slab and the pipe. It is understood from this figure that stiffness starts to decrease at applied load about 60tf, and the maximum load occurs at relative slip about 8mm. Ultimate shear strength of a stud of PS-1 and PS-2 is 5.68 and 5.67tf which agree with the 5.97tf calculated by Fisher formula. These results show that composite action is secured for the tube section by the stud type shear connectors.

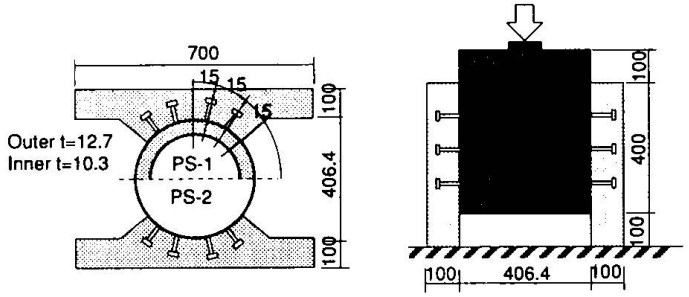

(a) Cross section *(b) Elevation*

Fig.9 Experimental methods and specimen

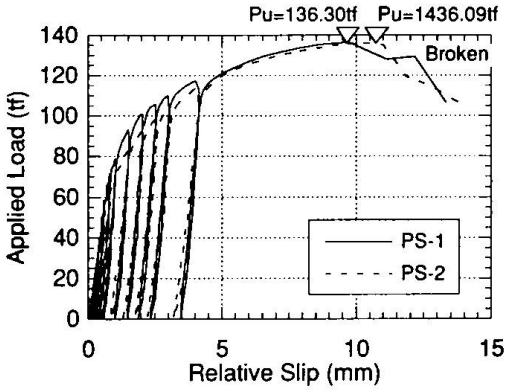

Fig.10 Load and relative slip curve

4. Noise Reduction Measurement

Noise and vibration levels of various girder sections are measured with the tapping device. Seven girder sections shown in fig.11 are tested: steel plate girder, steel plate girder with concrete panel attached, steel pipe, double steel pipe with concrete filled, steel pipe filled with air mortar with compressive stress of 7kg/cm^2, steel pipe filled with concrete and RC girder. Section modulus of all the sections are equal to compare on the equal basis. The tapping device shown in fig.12 consists of five hammers weighing 500g per each. The five hammers hit the concrete base on top of the specimen, at time interval of 100ms, with verocity of 88.5 cm/s. Microphones are set at 0.1m, 1m and 2m apart from the test specimen to catch the noise. Accelerometers are attached on three points of the specimen surface.

Noise levels collected by 0.1m microphone and acceleration levels on the surface are shown in

fig. 13. It is understood that the noise and acceleration levels have the similar tendency in all the cases. It is clearly shown that non-composite steel section, PN-1A and PN-2, have higher noise and acceleration levels than those of other composite sections. The air mortal filled pipe PN-4 is effective compared with non-composite sections, but the double pipe model PN-3 and concrete filled pipe PN-5 is more promising as good as concrete section PN-6. These experiments prove that concrete or mortar filling can reduce noise and vibration levels of steel pipe girders.

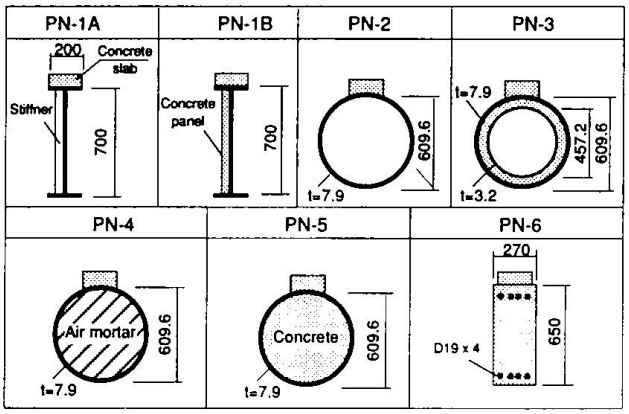

Fig.11 Test specimen

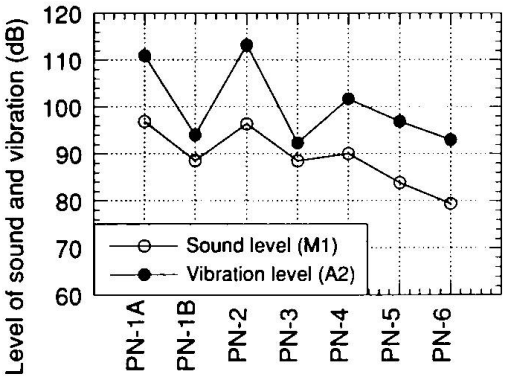

Fig.13 Measured data

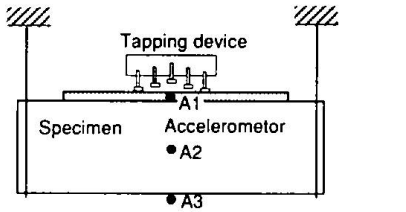

(a) Elevetion

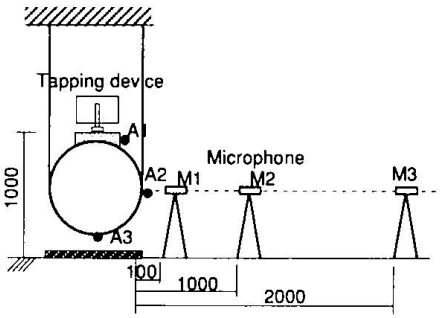

(b) Cross section

Fig.12 Measuring tools

5. Design of a New Railway Bridge

This new bridge system is proposed for railway bridges in the suburbs of Tokyo. Fig. 14 shows the general dimension of the bridge: five-span continuous girder bridge with each span-length of 20m. The deck level is about 10m above the ground. The bridge has two railways with train live load of 15 ton per wheel. Lateral force with 28% of dead loads is taken as seismic load.

Sub-structure consists of piles and columns. Piles are a new composite pile consistnig of steel pipes and soil cement with diameter of 1.2m and length of 19.4m. During the steel pipe is lowered with drilling device, cement milk is poured and mixed with soils inside the pipe. When the pile comes to the bottom position, base concrete is poured, and then the drilling device is pulled up. Spiral ribs are attached on the outer surface of the pile when it is rolled at the steel mill to increase the friction of pipe and soil cement solid. Major advantages of this new pile are quick installation, low noise level, and no removal of soil.

Concrete filled spiral pipes with diameter of 1.0m are used as columns. These pipes have good ductility and resistance against earthquakes. Ductile ratio up to 6 to 8 can be usually expected. A

column is inserted into a pile, and concrete are pored into the gap. The spiral ribs are attached on the outer surface of the column and the inner surface of the pile, which improve the friction and strengthen the joint. This pipe to pipe joint with concrete has been widely studied by Takano, Isibashi, Kamata and Kinoshita[1]. They carried out experiments and found that this connection has high initial rigidity, good ductile property, and high ultimate strength, when spiral ribs are attached on the surface and overlap length is over 1.5 D (D: column diameter).

The super-structure is the two pipe girder system with pipe diameter of 1.117m. Concrete is filled inside the pipe girder near the piers, where negative bending moment is dominant. Air mortal is filled inside the pipe girder around span center, where positive bending moment is dominant and therefore composite effects of girder and RC slab can be expected. The air mortar is expected to reduce the noise level, but is not expected in bending strength. The stab pipe with spiral ribs is welded to the girder at intermediate support, inserted into the column and connected to the column by the same method used as the pipe to pile connection. Prefabricated composite slab is used to support the train loads.

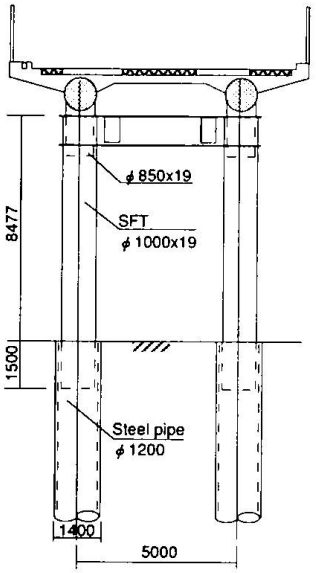

Fig.15 Sub-structure

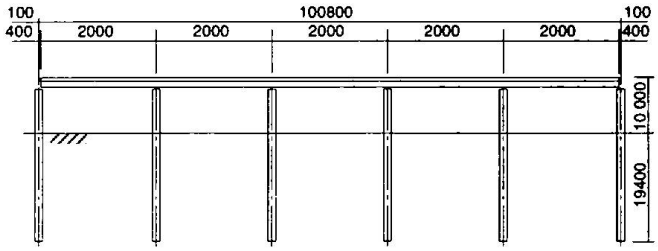

Fig.14 Layout of the new bridge

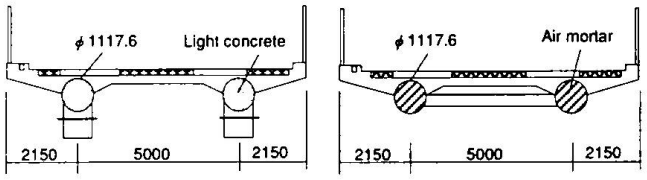

(a) Near support *(b) Span center*

Fig.16 Cross section of girders

6. Conclusion

The new railway bridge system using concrete or air mortar filled steel pipes are proposed and studied by analysis and experiments. The experiments show that the concrete filled steel pipes have high ultimate bending strength and good ductility. Air mortar with compressive stress over 50kg/cm^2 could improve ductile property. Concrete slab and pipe girder have adequate shear strength by using studs. These pipe girders could reduce noise and vibration levels induced by trains.

The construction methods and cost of this new bridge are investigated for the planned railway bridges. It is found that estimated construction period is only 14 months to complete one kilometer long bridges. The estimated construction cost is substantially lower than that of the conventional steel bridges. It is concluded from this study that this new railway bridge system is feasible and economical.

Reference

1)Takano, Ishibashi, Kamata & Kinosita: Column-pile joints made of steel pipes filled with concrete, Fourth World Congress on Joints and Bearings, September, 1996.

Design of High-Rise Building using Round Tubular Steel Composite Columns

Naoki UCHIDA
Associate Director
Nikken Sekkei Ltd
Osaka, Japan

Naoki Uchida, born on 1940, received his Doctor's degree from the graduate school of the Univ. of Tokyo where he majored in steel structure. He has been engaged in structural design for over 30 years.

Hirokazu TOHKI
Senior Structural Engineer
Nikken Sekkei Ltd
Osaka, Japan

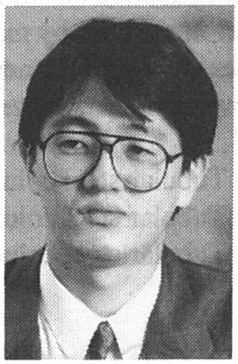

Hirokazu Tohki, born on 1962, He got his M.E. from Univ. of Kyoto. Since 1986, he has been engaged in structural design of buildings, awarded "JSCA award" form Japan Structural Construction Association in 1995.

Summary

This paper is a brief report on a specific case of building structural design wherein possible advantages of composite structures were pursued intensively. The paper will give at the outset an overview of the composite structures commonly used in Japan, then it will describe some advantages that may be expected from tubular steel composite columns (and also from high quality high strength steel used to form such composite columns), and finally the paper will describe the essence of the captioned structural design.

1. Composite Structures Commonly Used in Japan

Composite structures certainly have their own advantages; however, if their advantages are to be utilized to a full extent, the characteristics of each component must be used for a fitting purpose and all the component to display its intrinsic merits fully and to supplement at the same time any demerits of other components in order to ensure excellent structures. In Japan, structures are made "composite" at various levels and stages. For example, we have composite materials, composite members, composite structures and composite frames. Glass fiber reinforced concrete (known as GRC) which is composed of concrete mixed with glass fibers to give it some tensile strength may be cited as a case of making it "composite" at the material level. Structural members formed by structural steel combined with reinforced concrete which are extensively used in Japan, composite beams consisting of steel beams and reinforced concrete slabs, composite floors formed by factory-made precast concrete slabs combined with in-site concrete slabs and walls made in a similar manner are also very popular. At the structure level, composite structures are seen in which reinforced concrete members having high rigidity are combined with lightweight ductile steel members in forming vertical and horizontal elements. As regards framing types, large scale frame systems composed of "super frames" and "subframes," which are often used for very tall buildings may be taken as a good example of composite frames.

Among this variety of composite elements, this paper deals with composite columns formed by round tubular steel filled and covered with concrete.

2. Some Structural Advantages of Round Tubular Steel Composite Columns

Round tubular steel composite columns may be defined as composite columns made up of round steel tubes filled and covered with concrete. Having been considered as structural element which makes effective use of merits of each of its components, this type of columns have been studied rather intensively by many engineers for research and development. Composite columns made up of steel tubes and concrete may generally be divided according to their structural types into the following three categories as shown in Fig. 1.

(1) Tubular steel columns filled with concrete
(2) Tubular steel columns covered with concrete
(3) Tubular steel columns filled and covered with concrete

(1) Tubular steel columns filled with concrete (2) Tubular steel columns covered with concrete (3) Tubular steel columns filled and covered with concrete

Fig. 1 Types of Composite Column Structure

Since round steel tubes are simple in cross sectional shape, they can be readily filled and/or covered with concrete. Design advantages that can be expected from the round steel tubes used for columns and making them into composite columns are as enumerated below.

- Round Steel Tubes
  - Since they have non-directional cross sections, they can be expected to display enough bearing strength against lateral force applied to them in diagonal direction.
  - In case the columns are connected to girders in diagonal direction, connections can be detailed easily.
  - As basic material, round steel tubes have excellent industrial productivity.
  - Round steel tubes make it easier to utilize automatic welding by industrial robots in welding operation.

- Composite Columns
  - Composite effects help increase rigidity and strength of columns.
  - Local buckling of steel tubes can be avoided by the composite effects.
  - Fire resistance of steel columns is improved.

For these reasons, it is expected that the use of composite columns consisting of round steel tubes and concrete in high -rise buildings will further increase as buildings are diversified in types, material strength is increased and construction process is industrialized.

In the high-rise building described in the following paragraphs, columns composed of steel tubes in-filled and covered with concrete used. In the open space at the base of this building, composite columns formed by tubes made of high quality high strength steel having 590 N/mm^2 tensile strength (here in after reffered to as "high strength steel") and high strength concrete were employed.

The term "high quality high strength steel" is used here to mean such high tensile steel which displays comparatively little yield point variations and has a low yield ratio (i.e. a low yield point-tensile strength ratio). In other words, the term means high strength steel that shows high energy-absorbing performance. In earthquake-prone Japan, primary consideration must be given in building design to the building's behaviors during a seismic event. To cope with an extremely severe earthquake which rarely occurs, a design technique is used by which an appropriate parts of the frames are let to enter a plastic range in event of such an earthquake thus enabling seismic energies to be absorbed. Use of high quality high strength steel provides a positive means to absorb great energies, to minimize steel plate thickness and thus to enhance workability.

The case introduced here indicated that the use of composite columns formed by high strength steel tubes and high strength concrete is an effective way to enable columns to carry great axial loads.

3. A Case of A High-rise Building Using Tubular Steel Columns Filled and Covered with Concrete

3.1 Summary of Design

The building introduced here as an example is a high-rise building with a height of 101.2 m having 21 above ground floors and a basement. Creating "an up-to-date building in the high-tech age" and providing "bright and open office spaces commanding good views" were the primary design concepts. A typical floor plan consisting of the outside core and one-room type office spaces was adopted to ensure maximum space flexibility. Columns were at the mid-point of each exterior wall, and this was conductive to most attractive feature of this building, namely a building commanding nice views.

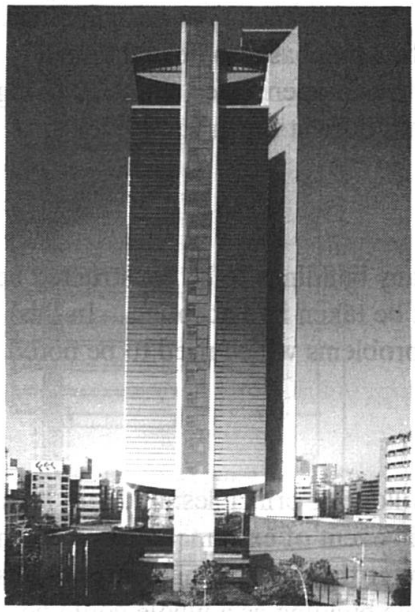

Fig. 2 External Appearance

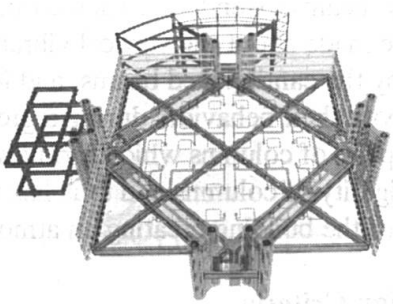

Typical Floor Framing Plan

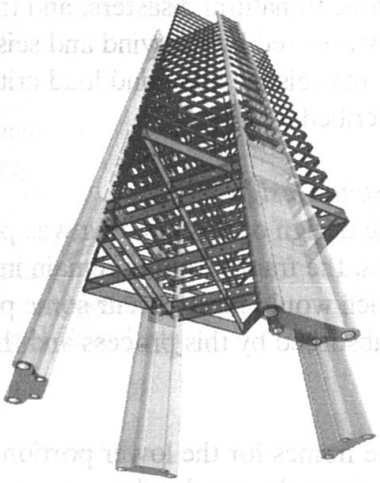

Fig. 3 Framing Perspectives

Structurally, this building is in the form of rigid frames composed of steel tubes filled and covered with concrete and structural steel beams. Each pair of columns is located at mid-point of each exterior wall and one pair of columns is connected to another pair of columns with a pair of bearing girders, thus forming the frames whose corners meet the exterior walls at an angle of 45°. These structural frames or "skeltons" also form utility skeltons. Namely, spaces within the three pairs of columns are used for air conditioning equipment rooms and spaces between pairs of girders are used as main chambers of air conditioning system. Two cross beams are located at each floor level in direction orthogonal to each pair of bearing girders and these cross beams are connected to cantilevered beams supporting exterior walls and floors. Floors are composed of precast concrete slabs of joist type each about 8 m in span. These slabs, free of small subbeams, ensure flexibility in providing piping under these slabs.

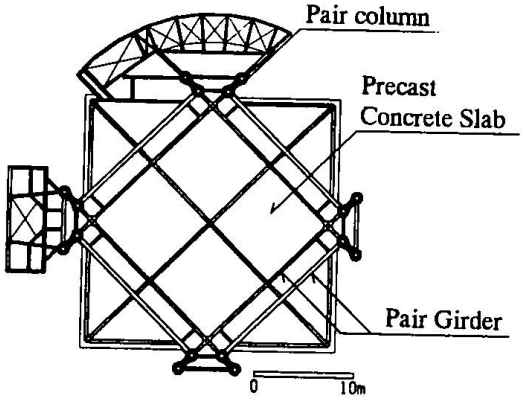

Fig. 4 Framing Plan

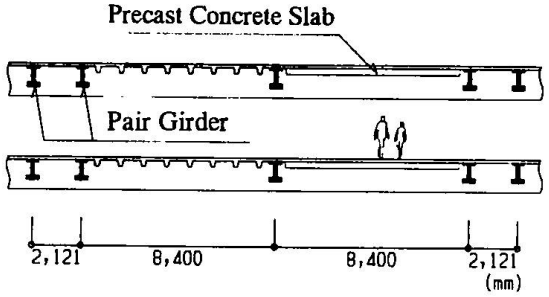

Fig. 5 Section of Typical Floor

Cantilevered beams extended to each corner of the building has a span of about 7 m. Careful studies were made about the vertical vibrations of the floor beams at the corners of the building supported by the cantilevered beams, and it was confirmed that these corners create no problems in respect of both their behaviors during a great seismic event and their habitability at normal times. The use of pairs of columns which form a visual feature of this building has also helped ensure structural rigidity of columns and thus has made it possible to provide open space about 20 m high at the base of the building creating an atmosphere open to the exteriors at the ground level.

3.2 Design Criteria

Japan is prone to natural disasters, and the structural design of any buildings to be constructed here is inevitably affected by the wind and seismic forces which must be taken into account. In this paragraph, the seismic and wind load criteria and some related problems which need to be noted will be described.

3.2.1 Seismic Design

The seismic design of this building was primarily based on the following principles: under moderate earthquakes, the frames should remain in the elastic range, and in event of extremely severe earthquakes which would rarely occur some parts of frames would enter the plastic range but energies would be absorbed by this process and thus serious damage to the building as a whole could be avoided.

Further, the frames for the lower portion (below the third floor level) which is designed as a large open space were designed to have some extra strength so that they would be able to withstand

severe earthquakes without damage. In the typical floors, too, the structural elements were so designed that only the beams outside pairs of girders would enter the plastic range while the beams inside them would remain in the elastic range, thus avoiding drastic change in rigidity of the building.

3.2.2 Wind Resistant Design

This building has a complicated configuration both in plan and in elevation. So, needs were felt to ascertain how the building would be structurally affected by its complicated shape. In particular, the structural behaviors of the fan-shaped north side portion where the building has a curved surface and a sharply cut-in part as well as a large open space were thought to require careful studies. Hence, a series of wind tunnel tests were reflected on the structural design.

Through these tests, it was ascertained that the open space at the base of the building could effectively reduce the winds induced by adjacent buildings. Also, in consideration that the existence of a sharply cut-in portion on the north side of the building might cause the building to be twisted by the wind force, such wind effects were ascertained by the wind tests and the design wind loads were determined accordingly.

3.3 Design of Pairs of Columns

A pair of columns located at the center of the exterior walls were made of steel tubes filled and covered with concrete. On the typical floors, round steel tubes (ϕ 660.4 mm) were connected with

H-shaped steel beams, steel tubes were in-filled with concrete, and then by covering both walls and columns integrally with concrete, pairs of columns were formed. Steel tubes were formed by bending a steel plate and ring-shaped forged steel diaphragms were used at joints.

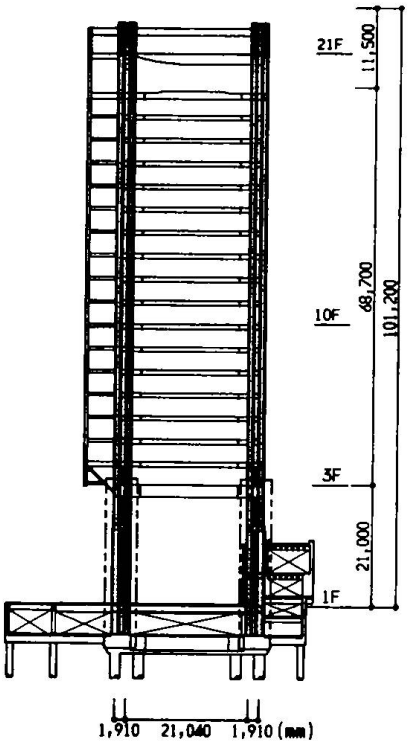

Fig. 6 Framing Elevation

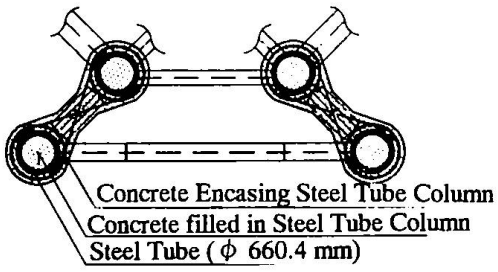

Fig. 7 Section of Pair Column (Typical Floor)

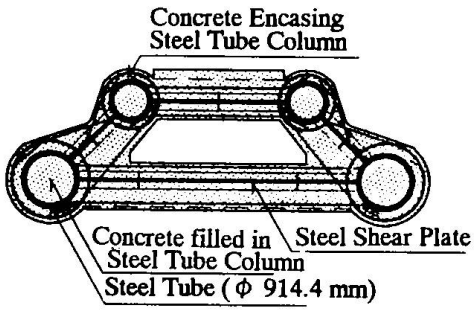

Fig. 8 Section of Pair Column (Large open space)

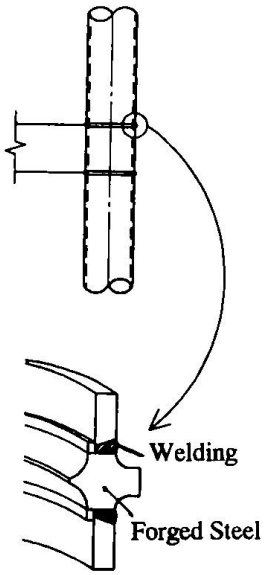

Fig. 9 Formation of Steel Column

The axial force acting on the pair columns in the open space amount to about 4,000 metric tons per pair. Hence, the frames below the third floor level forming a large open space were designed to have large bearing capacities so that they would be able to stay within the elastic range in event of a great earthquake. For the tubular steel columns in this space where they are subjected to high axial force and so must have high rigidity, steel tubes made of high strength steel were used in combination with high strength concrete to ensure the required bearing capacity and rigidity. The use of high strength steel made it possible to reduce the maximum plate thickness to 50 mm for steel tubes 914.4 mm in diameter (i.e., D/t = 18.2, D: diameter t: thickness), and this certainly helped enhance workability, weldability and economy of the connection.

As has been already mentioned, round steel tubes have a shape which is adaptable for automatic welding by means of industrial robots. For construction of this building, robots were used in both factory welding and field welding for column connection.

Placement of concrete into steel tubes was conducted by the use of tremies for each nit height of a column (i.e., equal to the height of three floors or about 12 m).

4. Conclusive Remark

This paper describes the design of a high-rise office building in which pairs of round steel tube (made of high strength steel) composite column were used. The writers believe that a unique and dynamic piece of architecture was realized in this project by using high quality high strength steel and round steel tube composite columns to the best advantage. Further, they expect that the use of high strength steel and high strength concrete in an appropriate combination will expand the potential area of structural design and that this paper indicates such potentiality.

References

1) Fumio OHTAKE, Tsugio IIDA, Koji FUKUDA, Naoki UCHIDA, Akira HANAJIMA, Hirokazu TOHKI, "Beam-Column Connection Test of Concrete filled Circular Column made of High Quality 60 kg/mm^2 Tensile Strength Steel Tube", Journal of Structural Engineering, Vol.39B, 1993., Japanese Society of Steel Construction

2) Akira HANAJIMA, Hirokazu TOHKI, Haruo TSUKAGOSHI, Saburo KAWABATA, "Wind-Resistant Design for Buildings with Complicated Configuration", The 12th National Symposium on Wind Engineering, 1992., Japan Association for Wind Engineering

3) Architectural Institute of Japan, Guidelines for the Evaluation of Habitability to Building Vibration, 1991.

4) Naoki UCHIDA, Akira HANAJIMA, Hirokazu TOHKI, "Use of High-quality, High-strength Steels in Design of a High-rise Building", Journal of Steel Construction Engineering, Vol.1, No.1, 1994, Japanese Society of Steel Construction

6) Akira HANAJIMA, Hirokazu TOHKI, Haruo TSUKAGOSHI, "Study on Vibratory Characteristics of Large, Cantilevered Floor Structure", Journal of Architecture and Building Science, Vol.3, 1996, Architectural Institute of Japan